

# Isosteviol Sodium Exerts Anti-Colitic Effects on BALB/c Mice with Dextran Sodium Sulfate-Induced Colitis Through Metabolic Reprogramming and Immune Response Modulation

Shanping Wang<sup>1</sup>  
Jiandong Huang<sup>1</sup>  
Fei Liu<sup>1</sup>  
Keai Sinn Tan<sup>2,3</sup>  
Liangjun Deng<sup>1</sup>  
Yue Lin<sup>1</sup>  
Wen Tan<sup>3,4</sup> 

<sup>1</sup>Institute of Biomedical and Pharmaceutical Sciences, Guangdong University of Technology, Guangzhou, People's Republic of China; <sup>2</sup>College of Pharmacy, Jinan University, Guangzhou, People's Republic of China; <sup>3</sup>Post-Doctoral Innovation Site, Jinan University, Yuanzhi Health Technology Co, Ltd, Zhuhai, People's Republic of China; <sup>4</sup>Jeffrey Cheah School of Medicine and Health Sciences, Monash University Malaysia, Bandar Sunway, Malaysia

**Purpose:** Inflammatory bowel diseases (IBDs) are global health problems that are associated with immune regulation, but clinical IBDs treatment is currently inadequate. Effective preventive or therapeutic methods for immune disorders rely on controlling the function of immune cells. Isosteviol sodium (STV-Na) has antioxidant activity, but the therapeutic effect of STV-Na against IBD remain undocumented. Herein, we investigated the therapeutic effect of STV-Na in mice models with IBDs.

**Methods:** Mice received 3.5% DSS for 7 days to establish IBD models. Intraperitoneal STV-Na was given 2 days before DSS and lasted for 9 days. Commercially available drugs used in treating IBDs (5-aminosalicylic acid, dexamethasone, and infliximab) were used as positive controls. Samples were collected 7 days after colitis induction. Histopathological score, biochemical parameters, molecular biology methods, and metabolomics were used for evaluating the therapeutic effect of STV-Na.

**Results:** Our data revealed that STV-Na could significantly alleviate colon inflammation in mice with colitis. Specifically, STV-Na treatment improved body weight loss, increased colon length, decreased histology scores, and restored the hematological parameters of mice with colitis. The untargeted metabolomics analysis revealed that metabolic profiles were restored by STV-Na treatment. Furthermore, STV-Na therapy suppressed the number of CD68 macrophages and F4/80 cell infiltration. And STV-Na suppressed M1 and M2 macrophage numbers along with the mRNA expressions of proinflammatory cytokines. Moreover, STV-Na administration increased the number of regulatory T (Treg) cells while decreasing Th1/Th2/Th17 cell counts in the spleen. Additionally, STV-Na treatment restored intestinal barrier disruption in DSS-triggered colitis tissues by ameliorating the TJ proteins, increasing goblet cell proportions, and mucin protein production, and decreasing the permeability to FITC-dextran, which was accompanied by decreased plasma LPS and DAO contents.

**Conclusion:** These results indicate that STV-Na can ameliorate colitis by modulating immune responses along with metabolic reprogramming, and could therefore be a promising therapeutic strategy for IBDs.

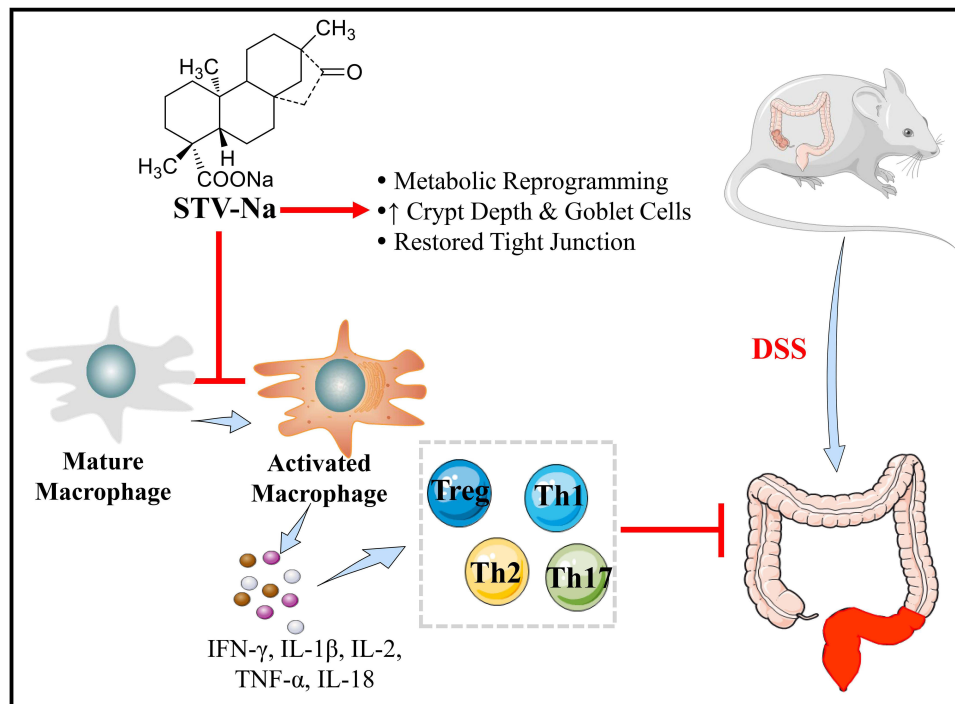
**Keywords:** inflammatory bowel disease, isosteviol sodium, macrophage polarization, Th cells, barrier function, metabolomics

Correspondence: Wen Tan  
Post-Doctoral Innovation Site, Jinan University, Yuanzhi Health Technology Co, Ltd, Hengqin New District, Zhuhai, People's Republic of China  
Tel/Fax +86 20-85827854  
Email uscnwt@163.com

## Introduction

The hallmarks of inflammatory bowel diseases (IBDs), which comprise Crohn's disease (CD) and ulcerative colitis (UC), are chronic, persistent, and recurrent

## Graphical Abstract



intestinal ulcers. IBDs have been classified as modern refractory diseases by the WHO.<sup>1</sup> The one of common clinical manifestation of IBDs is refractory colonic bleeding from ulcerations resulting from the erosion of blood vessel, which invariably leads to iron deficiency anemia.<sup>2</sup> Millions of patients around the world suffer tremendously from IBD, leading to insurmountable socioeconomic losses.<sup>3</sup> To date, the pathogenesis of IBDs has been incompletely elucidated, in part due to the complex nature of these diseases. IBDs are thought to involve genetic susceptibility, external environmental stimulation, host immune dysfunction, metabolic disorder, and intestinal mucosal barrier damage.<sup>4,5</sup> The microbiome invading intestinal tissues during injury trigger a strong immune response leading to excessive inflammatory cytokines release, which propagates the disease.<sup>6</sup> IBDs have been thought to be primarily mediated by macrophages.<sup>7</sup> Macrophages are able to be induced into two primary polarities, namely the classically activated macrophages (M1 phenotype) and alternatively activated macrophages (M2 phenotype). Upon injury, inflammation induces the formation of M1 macrophages. Once the injury stabilizes, inflammation is halted by M2 macrophages.<sup>8</sup> Activation of the immune response in turn impairs the intestinal

epithelial barrier function by reducing the number of tight junction (TJ) proteins, further promoting inflammation.<sup>9</sup> Therefore, IBD treatment revolves around inflammation suppression and control as well as mucosal barrier repair.

In addition to macrophages, the adaptive immune system heavily features T helper (Th) cells. Naïve T cells are able to differentiate into a myriad of effector T cells such as Treg cells, Th1, Th2, and Th17 cells, releasing a plethora of cytokines specific to each T cell subtype. Chronic inflammation in IBDs is marked by a pro-inflammatory cellular milieu in addition to dysfunctional T cell responses. The development and progression of IBDs hinges on the delicate balance between anti- and pro-inflammatory cytokines. Imbalances in the Th1/Th2/Th17/Treg cell numbers are considered to be an essential cause of IBDs.<sup>10,11</sup> Additionally, a series of proinflammatory factors, such as interleukin (IL)-1β, interferon-γ (IFN-γ), and tumor necrosis factor-α (TNF-α), are released in IBDs and contribute to disease progression.<sup>12</sup> Therefore, anti-inflammatory drugs (5-aminosalicylic acid (5-ASA) and corticosteroids (dexamethasone, Dex)), anti-TNF-α monoclonal antibodies (infliximab (IFX)), and immunosuppressive agents (vedolizumab) are frequently used for the

treatment of IBDs.<sup>13,14</sup> However, these drugs are expensive and result in severe and debilitating side effects, such as systemic immunosuppression, kidney toxicity, diabetes, weight gain, and hypertension.<sup>13,15</sup> Therefore, novel therapeutic agents with fewer undesirable adverse reactions are necessary. Recently, several natural plants, including indigo,<sup>16</sup> berberine,<sup>17</sup> and rutaecarpine,<sup>18</sup> have demonstrated promising therapeutic effects and safety profiles when used to treat IBDs. However, the exact therapeutic mechanisms of these natural products remain poorly understood. Moreover, the metabolic consequences of current therapeutic agents used to treat IBD have not been comprehensively analyzed.

Recent evidence indicates that metabolic disorders critically modulate the pathogenesis of IBDs by activating intestinal immune cells. Thus, investigating whether colitis can be alleviated by inducing metabolic changes would be meaningful.<sup>5,19</sup> Furthermore, researchers have successfully elucidated the potential targets and mechanisms underlying candidate drugs in specific diseases through metabolomics approaches.<sup>20,21</sup> UHPLC-TIMS-TOF-MS/MS (ultrahigh-performance liquid chromatography combined with trapped ion mobility spectrometry coupled to time of flight tandem mass spectrometry), is a means of analyzing metabolic profiles as it exhibits a high resolution and sensitivity in measuring plasma levels of metabolites. Therefore, our study seeks to determine the metabolic changes in colitis undergoing treatment in an effort to identify novel pathways that may be targeted by novel agents.

Isosteviol sodium (STV-Na, [Figure 1A](#)) is a natural terpenoid derived from stevioside, a plant belonging to the *Stevia rebaudiana* composite family. Previous studies have demonstrated the antiapoptotic and antioxidant effects of STV-Na.<sup>22,23</sup> STV-Na protects against diabetic myocarditis,<sup>22</sup> exhibits anti-myocardial ischemic activity, and yields a significant anti-myocardial ischemia effect.<sup>24</sup> However, the therapeutic value and underlying mechanism of action of STV-Na against IBD remain unclear. This series of investigations seeks to understand the therapeutic effect of STV-Na against IBDs by employing a dextran sulfate sodium (DSS)-induced IBD mouse model. Our data demonstrate that STV-Na can alleviate colitis by regulating inflammatory activity, the immune response and metabolic reprogramming. This study provides a new treatment option and novel therapeutic strategy for IBDs.

## Materials and Methods

### Chemicals and Reagents

STV-Na was supplied by Key-Pharma Biological Inc. (Dongguan, China). The 5-ASA and Dex were procured from Shanghai Yuanye Bio-Technology Co., Ltd (Shanghai, China); infliximab was obtained from Pfizer Pharmaceuticals Ltd (Janssen Biotech, Horsham, PA, USA); fluorescein isothiocyanate (FITC)-dextran (average molecular weight (mw) 4000) was purchased from Sigma-Aldrich (St. Louis, MO, USA); DSS (mw 36,000–50,000), the MolPure<sup>®</sup> Cell/Tissue Total RNA Kit, Hieff UNICON<sup>®</sup> Universal Blue qPCR SYBR Green Master Mix and Hifair<sup>®</sup> III 1st Strand cDNA Synthesis were obtained from Yeasen Biotech (Shanghai, China); the Th1/Th2/Th9/Th17/Th22/Treg Cytokine 17-Plex Mouse ProcartaPlex<sup>™</sup> Panel was purchased from ThermoFisher Scientific (Waltham, MA, USA); a mouse lipopolysaccharide (LPS) ELISA kit and mouse diamine oxidase (DAO) activity assay kit were obtained from Cusabio Biotech Co. Ltd. (Hubei, China); Alexa Fluor 488 anti-mouse CD3, Brilliant Violet (BV)-605 anti-mouse CD4, BV-711 anti-mouse CD25, PE/Dazzle 594 anti-mouse IFN- $\gamma$ , BV-421 anti-mouse IL-4, BV-510 anti-mouse IL-17A, phycoerythrin (PE) anti-mouse Foxp3, PE anti-mouse F4/80, BV-421 anti-mouse CD11c, FITC anti-mouse CD206, and cell activation cocktail (with Brefeldin A) were bought from BioLegend Company (San Diego, CA, USA); Anti-CD86 antibody (bs-1035R) and anti-CD163 antibody (bs-2527R) were obtained from Bioss Biotechnology (Bioss, Beijing, China). An anti-ZO-1 primary antibody was acquired from Affinity Biosciences (Cincinnati, OH, USA); an anti-MUC2 primary antibody was procured from Santa Cruz Biotechnology (Santa Cruz, CA, USA); and an anti-claudin-1 primary antibody was procured from Abcam (Cambridge, MA, USA). The highest analytical grade reagents were utilized for these experiments.

### Animals

Male BALB/c mice (6 to 8 weeks old; weighing 20 to 22 g) were obtained from the Guangdong Medical Laboratory Animal Center (Guangzhou, China). All mice were allowed to acclimatize for a week before any experiments were performed under specific pathogen-free conditions comprising 50–55% humidity, a 12-h light/12-h dark cycle, and a temperature of 24–25 °C. Food and water were provided *ad libitum*. The Guide for the Care and Use of Laboratory Animals (National Institutes of Health, USA) was closely

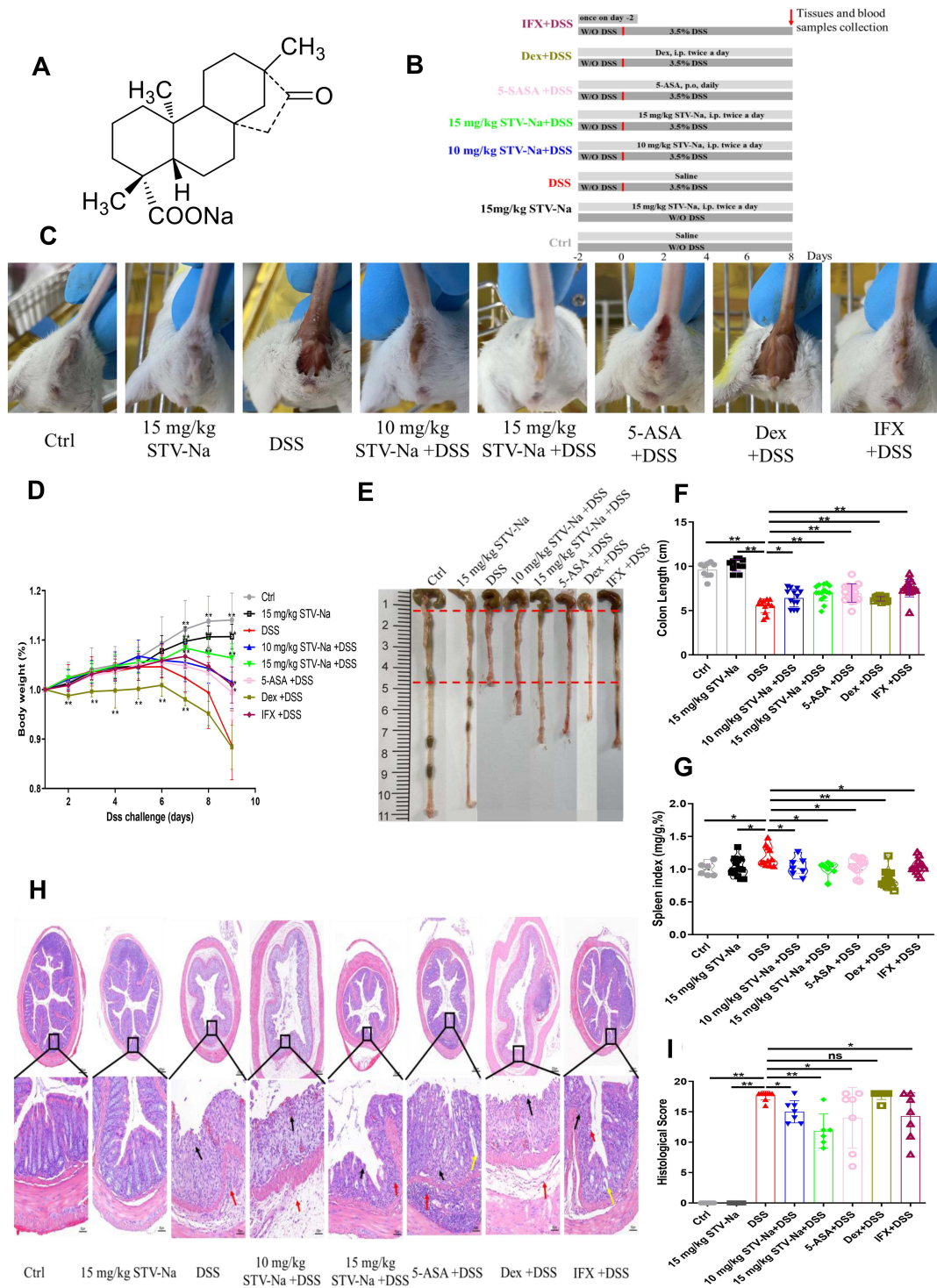


**Figure 1** STV-Na protects mice against IBDs. Male Balb/c mice were intraperitoneally administered 10 mg/kg or 15 mg/kg STV-Na or normal saline twice daily for two consecutive days from days -2 to 7 and fed drinking water supplemented with 3.5% (w/v) DSS *ad libitum* from days 0 to 7. **(A)** Chemical structure of STV-Na. **(B)** Schematic diagram of the experiment. **(C)** Representative bloody stool samples from mice. **(D)** The body weight was measured daily. Data are charted in terms of percentages of basal body weight. **(E)** Colonic tissue samples. The distance between the red dotted line indicates the length of the colon. The colon length of the DSS model group is the shortest among different groups. **(F)** Length of the colon (cm) in the different groups was measured at the end of the experiment. **(G)** Spleen weight to body weight ratio. **(H)** Representative photographs of whole colon sections stained with H&E. Scale bars, 200  $\mu$ m (50  $\mu$ m in the magnified images). The arrows indicate inflammatory cell infiltration (red), crypt architectural abscess and distortion (yellow), and epithelial ulceration and erosion (black). **(I)** Histological scores of the H&E stained sections. Data are published in terms of means $\pm$ SDs. The statistical analyses were performed with Student's t-test or one-way ANOVA followed Turkey's post hoc test (n = 6 to 12 mice per group; each data point represents one mouse); \*P < 0.05 and \*\*P < 0.01 in contrast to the DSS group. **Abbreviation:** ns, not significant.

adhered to in the formulation of all animal experimental procedures. All experimental animal protocols were passed by the Institutional Animal Care and Use Committee of Sun Yat-sen University, Guangzhou, China (Ethical Approval No. IACUC 20140515171141).

The mice were arbitrarily split into 8 cohorts (Figure 1B): (1) the control group, (2) the STV-Na reference (15 mg/kg) group, (3) the DSS group, (4, 5) two DSS+STV-Na (10 and 15 mg/kg) groups, (6) the DSS+5-ASA (50 mg/kg) group, (7) the DSS+Dex (0.25 mg/kg) group and (8) the DSS+IFX (10 mg/kg) group. To further unravel the protective mechanisms of STV-Na when used to treat DSS-induced colitis, control mice were administered intraperitoneal saline, and those in the DSS+STV-Na group received intraperitoneal STV-Na dissolved in saline twice per day from days -2 to 7. The mice of the DSS and DSS+STV-Na groups were fed 3.5% (wt/vol) DSS in their drinking water, which was provided *ad libitum*, from days 0 to 7 to induce acute colitis, according to the methods published by Li et al.<sup>25</sup> The 5-ASA, Dex, and IFX were used as positive control drugs and administered to the mice at dosages corresponding to those used clinically.<sup>26–28</sup> The 5-ASA was administered daily via intragastric methods from day -2 to day 7. The administration dosage, method and time of STV-Na treatment were chosen based on the literature.<sup>29,30</sup> Dex was intraperitoneally injected twice a day from day -2 to day 7, and IFX was injected into the peritoneum once on day -2. The mice in the control and DSS groups were intraperitoneally administered the same volume of PBS. The body weight of all mice was monitored daily. On day 8, mice were sacrificed and their colon lengths were measured. The whole blood was obtained and centrifuged at 2000 g for 15 min at 4°C to collect plasma samples. The spleens were removed aseptically and weighed, and plasma, spleen, and colon tissues were stored for further analysis.

## Intestinal Permeability

Fluorescein isothiocyanate-dextran (FITC-dextran) (4 kDa, Sigma Aldrich, USA) was used to assess intestinal permeability, based on methods from a previous publication.<sup>31</sup> Briefly, the mice were fasted overnight and intragastrically infused with FITC-dextran at a dose of 500 mg/kg. Blood samples were drawn after 6 h, with serum samples collected upon centrifuging whole blood at 4 °C and 5000 rpm for 10 min. An equal volume of PBS (pH 7.4) was used to dilute the serum before a SpectraMax M3 microplate reader (Molecular Devices, Sunnyvale,

CA, USA) with an excitation wavelength of 485 nm and an emission wavelength of 520 nm was used to analyze the FITC-dextran concentrations, which were calculated based on a standard curve generation using PBS-diluted FITC-dextran (concentrations of 0, 125, 250, 500, 1000, 2000, 4000, 6000, and 8000 ng/mL).

## Hematological Analysis

Blood sample was collected from each group in an EDTA-containing tube at the end of the experiment. Hematological parameters were determined using an IDEXX ProCyte DX hematology analyzer (IDEXX, Westbrook, ME, USA). Measured parameters included red blood cell (RBC) counts, hematocrit (HCT), hemoglobin (HGB), monocytes (MONO), lymphocytes (LYMPH), and total white blood cell (WBC) counts.

## Metabolomics

An untargeted metabolomic profiling of plasma samples was performed as described in our previous publication.<sup>32,33</sup> Progenesis QI V2.4 (Waters Corporation, Milford, MA, USA) was used to remove background disruptions from the data before it was normalized against a reference sample (probabilistic quotient normalization), corrected to peak selection and retention times. Multivariate statistical analyses, including orthogonal partial least squares-discriminant analysis (OPLS-DA), partial least squares-discriminant analysis (PLS-DA), and principal component analysis (PCA) allowed us to identify the altered compounds in each group. Metabolites that were most likely to explain metabolome variance among the control, DSS, STV-Na, 5-ASA, Dex and IFX groups were identified using OPLS-DA. Variables with fold change (FC) values > 2, variable importance in projection values (VIP) > 1, and  $p < 0.05$  were considered candidate metabolites. The accurate mass and MS/MS spectra of the candidate metabolites were then contrasted against entries in the METLIN database ([www.metlin.scripps.edu/](http://www.metlin.scripps.edu/)), Lipid Maps (<http://www.lipidmaps.org>), and Human Metabolome Database (HMDB, <http://www.hmdb.ca/>) to identify potential biomarkers. MetaboAnalyst 5.0 (<https://www.metaboanalyst.ca>) was used to perform the pathway analysis.

## Cytokine Microarray Assay

High-throughput liquid protein chips (Luminex 200, USA) were used to evaluate mouse serum. The Th1/Th2/Th9/Th17/Th22/Treg Cytokine 17-Plex Mouse ProcartaPlex™

Panel (EPX170-26087-901, Thermo Fisher Scientific) allowed the quantification of: GM-CSF, IFN- $\gamma$ , IL-1 $\beta$ , IL-2, IL-4, IL-5, IL-6, IL-12p70, IL-13, IL-18, TNF- $\alpha$ , IL-9, IL-10, IL-17A, IL-22, IL-23, and IL-27. Not all analytes could be detected. Specifically, five cytokines were detected in this study. The cytokines in the samples were detected accordance to instructions stipulated by the manufacturer.

## Flow Cytometric Analysis

To determine the proportion of macrophages existing as different phenotypes (M0, M1, and M2) among spleens, splenocytes were treated with BV-421 anti-mouse CD11c antibody (117330), FITC anti-mouse CD206 antibody (141704) and PE anti-mouse F4/80 antibody (123110) (BioLegend, San Diego, CA, USA). The T helper (Th1/Th2/Th17/Treg) cell population was assessed by first stimulating splenocytes with BD GolgiPlug (550583) (BD Bioscience, San Jose, CA, USA) and a leukocyte activation cocktail for 6 h. Stimulated cells were then incubated with Alexa Fluor 488-conjugated anti-mouse CD3 (100210), BV-605-conjugated anti-mouse CD4 (100548), BV-711-conjugated anti-mouse CD25 (102038), PE/Dazzle 594-conjugated anti-mouse IFN- $\gamma$  (505846), BV-421-conjugated anti-mouse IL-4 (504127), BV-510-conjugated anti-mouse IL-17A (506933), and PE-conjugated anti-mouse Foxp3 (320008) antibodies (BioLegend, San Diego, CA, USA). A FACS Celesta flow cytometer (BD Bioscience, San Jose, CA, USA) was then used to evaluate fractions of macrophage phenotypes and Th cells.

## Real-Time Quantitative Polymerase Chain Reaction (RT-qPCR)

Total colonic RNA was isolated with the help of the MolPure<sup>®</sup> Cell/Tissue Total RNA Kit (Yeasen Biotech, Shanghai, China). cDNA was reverse transcribed using the Hifair<sup>®</sup> III 1st Strand cDNA Synthesis kit (Yeasen Biotech, Shanghai, China) and quantified with a real-time PCR system (LightCycler 96, Roche, Germany) using qPCR SYBR Green Master Mix. The  $2^{-\Delta\Delta C_t}$  method was used to assess relative gene expression levels. Rpl32 was used as an endogenous control because its expression is stable throughout gut inflammation. [Supplementary Table 1](#) lists all the primer sequences used.

## Measurement of LPS and Diamine Oxidase (DAO)

The serum LPS levels and DAO activity were quantified with commercial kits based on included manufacturer protocols (Cusabio Biotech Co. Ltd, Hubei, China).

## Alcian Blue-Periodic Acid-Schiff (AB-PAS) Staining of Colon Tissues

The depth of crypts and number of goblet cells were observed under a microscope, measured and counted using Image-Pro Plus software 6.0 (Media Cybernetics, Inc., Rockville, VA, USA) after cells were stained with AB-PAS.

## Histology, Immunohistochemistry (IHC) and Immunofluorescence (IF)

The distal colon (2–3 cm from the anus) was fixed in 10% neutral-buffered formalin, paraffin embedded, and used to produce 5 mm-thick sections. Hematoxylin and eosin (H&E) were used to stain samples which were then scored with a blinded scoring system ([Supplementary Table 2](#)). For IHC staining, paraffin-embedded colon fragments were processed using a standard IHC protocol. Briefly, the slides were incubated with rabbit antibodies against ZO-1 (1:100) (AF5145, Affinity Biosciences, Cincinnati, OH, USA), MUC2 (1:100) (sc-59859, Santa Cruz Biotechnology, CA, USA) or claudin-1 (1:100) (ab15098, Abcam Company, Cambridge, MA, USA). Immunodetection was accomplished with diaminobenzidine (DAB) reagent (DAKO ChemMate, DK). The expression of colonic tissue claudin-1, MUC2, and ZO-1 was semi-quantified based on the ratio of the integrated optical density (IOD) to the area (within at least three fields in each section) using Image Pro Plus 6.0 software (Media Cybernetics, Inc., Rockville, VA, USA). For IF staining, slides were incubated with primary antibodies (F4/80 (1:1000), CD86 (1:500), CD163 (1:300)) and with secondary antibodies for 1 h at room temperature. The 4', 6-diamidino-2-phenylindole (DAPI) used to counterstain nuclei. The fluorescence was visualized using a fluorescence microscope.

## Statistical Analysis

All data are depicted in terms of mean  $\pm$  SDs. Using the GraphPad prism 5.0 software (GraphPad Software Inc., San Diego, CA) was analyzed with either the Student's *t*-test or one-way ANOVA followed by Tukey's post hoc analysis test. Statistical significance was granted when the P value was  $<0.05$ . Multivariate data analysis carried out using EZinfo 3.0 (Waters Corporation, Milford, MA, USA). Significant p values

related to metabolite abundances gained using untargeted metabolomics were analyzed by one-way ANOVA and adjusted using the Benjamini-Hochberg FDR method with Progenesis QI.

## Results

### STV-Na Ameliorates IBD-Associated Phenotypes

Oral administration of DSS destroys the integrity of the colonic epithelial barrier, allowing it to become permeable to bacterial influx and thereby stimulating inflammation.<sup>1</sup> To evaluate the effect of STV-Na on IBDs, male BALB/c mice were exposed for 7 days to 3.5% DSS and received STV-Na (10 and 15 mg/kg, i.p. twice a day from day -2 to day 7), 5-ASA (75 mg/kg, P.O. daily from day -2 to day 7), Dex (0.25 mg/kg, i.p. twice a day from day -2 to day 7) or IFX (10 mg/kg, i.p. once on day -2). During the experimental process, DSS treatment caused more severe hematochezia and higher weight loss in all groups in contrast to the control mice. In line with a previous report,<sup>10</sup> our study showed that DSS-induced colitis could mimic the clinical symptoms of human IBDs. Furthermore, STV-Na, 5-ASA, or IFX significantly relieved the IBD symptoms, whereas the mice in the Dex group continued to show bloody stools and weight loss, and these symptoms were more severe in this group than in the DSS group. (Figure 1C and D). Mice with DSS-induced colitis exhibited a shorter colon length than control mice (Figure 1E and F), and STV-Na, 5-ASA, Dex, and IFX significantly abated this colon shortening.

Splenomegaly is often observed in patients with IBDs, and spleen weight is defined as an index of phenotyping systemic inflammation.<sup>34,35</sup> Consistent with previous studies,<sup>36</sup> enlarged spleens were observed in mice with DSS-induced colitis. As expected, STV-Na, 5-ASA, Dex, and IFX markedly reversed splenomegaly in mice with colitis (Figure 1G). A histological analysis of the distal colon demonstrated significant mucosal infiltration of inflammatory cells (Figure 1H). Colonic edema, crypt distortion and reduced number of goblet cells were observed in mice with colitis (Figure 1H). Notably, STV-Na, 5-ASA, and IFX treatments all induced notable histological improvements in crypt architecture and reduced levels of edema, mucosal injury and inflammatory cells infiltration. Compared with the DSS group, the histopathological scores were significantly and dose-dependently decreased in the DSS+STV-Na groups and

the effects in these groups were notably better than those that were treated with 5-ASA or IFX (Figure 1I). In contrast, Dex did not improve or even aggravate histopathological damage.

In summary, the STV-Na reference group demonstrated no apparent weight loss, change in the colon length, or histopathological damage in contrast to the control group. These results indicated that STV-Na effectively reversed the colitis progression in a dose-dependent manner and that its efficacy is superior to that of Dex and 5-ASA.

### STV-Na Attenuates Intestinal Inflammation in DSS-Induced Colitis

Hematological parameters have shown diagnostic importance in inflammation. As shown in Figure 2A–G, the DSS group displayed approximately twice as many white blood cells (WBCs) in contrast to the control group. Among WBCs, neutrophils (NEUTs), lymphocytes (LYMPHs), monocytes (MONOs), red blood cells (RBCs), hemoglobin (HGB), and hematocrit (HCT) were susceptible to DSS administration, as demonstrated by approximately 2.60-, 1.34-, and 3.06-fold higher and 0.87-, 0.87-, and 0.84-fold lower levels, respectively, in the DSS group than in the control group. Hematological parameters, such as WBCs, NEUTs, LYMPHs, and MONOs, markedly improved following STV-Na, 5-ASA, and IFX treatment.

Cytokines play essential roles in the etiology of IBDs. To investigate the systemic inflammatory pathways induced by gut inflammation, we quantified 17 inflammation-related cytokines. Among the 17 cytokines, five pro-inflammatory cytokines, namely, IFN- $\gamma$ , IL-1 $\beta$ , IL-2, TNF- $\alpha$ , and IL-18, were consistently identified in the serum of DSS-treated mice (Figure 2H–L). The serum levels of IFN- $\gamma$ , IL-1 $\beta$ , IL-2, TNF- $\alpha$ , and IL-18 in the DSS group were elevated approximately 1–3 times in contrast to those in the control group, and STV-Na significantly suppressed the DSS-induced burst of these pro-inflammatory cytokines. A similar reduction in IFN- $\gamma$  was observed following 5-ASA and IFX treatment. It is worth noting that IFX exhibited a significant inhibitory effect on TNF- $\alpha$ , whereas Dex did not significantly change the release of these cytokines. These results suggested that STV-Na alleviated inflammation in mice with DSS-induced colitis. Overall, we successfully established a colitis model and demonstrated that STV-Na ameliorated inflammation in IBD in a dose-dependent manner.

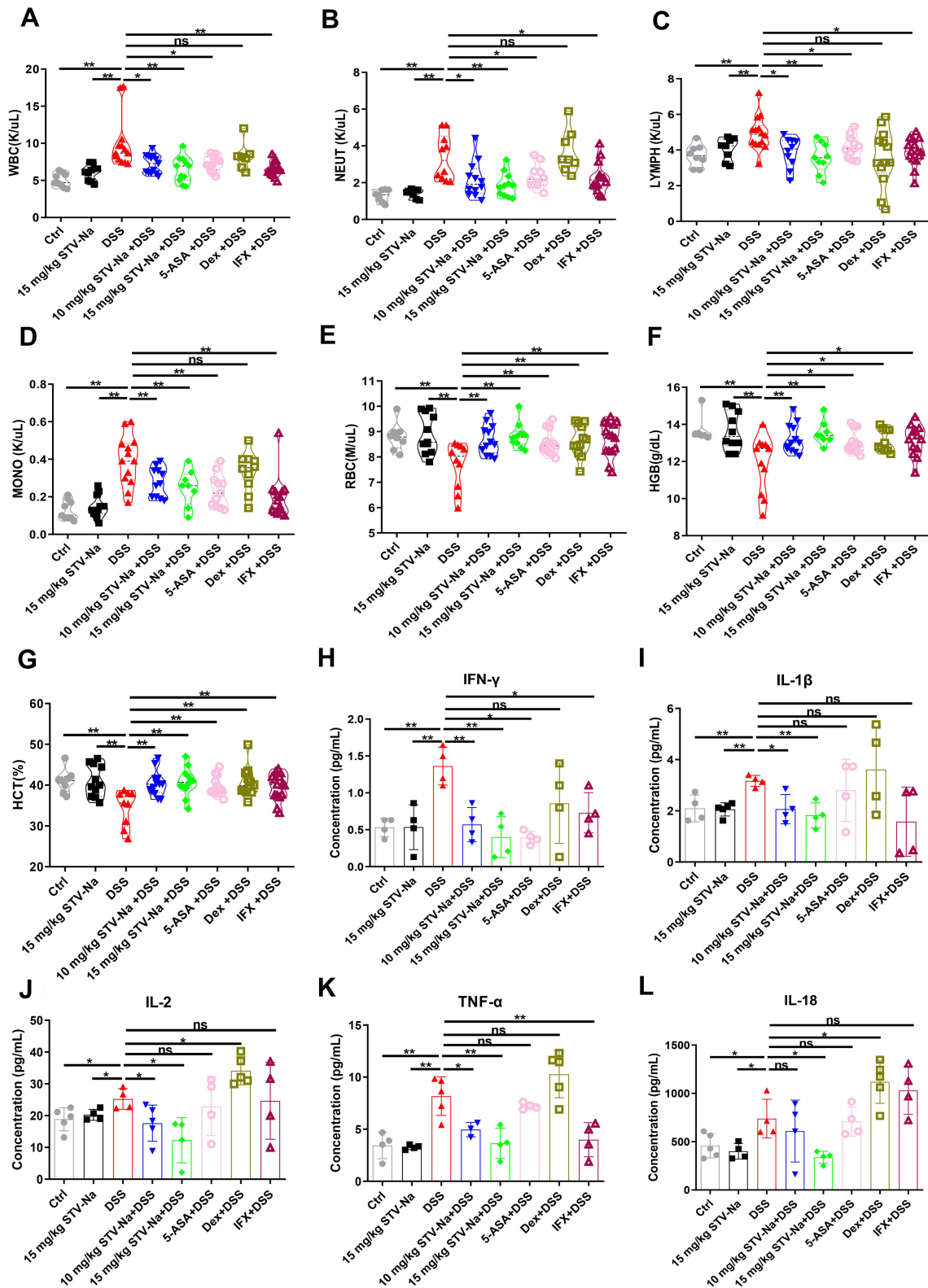


**Figure 2** STV-Na ameliorates inflammation of DSS-triggered colitis in mice. (A–D) The following hematological parameters were determined from the whole blood of mice: the numbers of WBCs (A), NEUTs (B), LYMPHs (C), MONOs (D), RBCs (E), HGB (F), and HCT (G). (H–L) Mice serum was evaluated for multiple inflammatory cytokines using the Cytokine 17-Plex Mouse ProcartaPlex™. Data are published in terms of means  $\pm$  SDs. The statistical analyses were performed with Student's *t*-test or one-way ANOVA followed Turkey's post hoc test ( $n = 4$  to 12 mice per group; each data point represents one mouse); \* $P < 0.05$  and \*\* $P < 0.01$  in contrast to the DSS group.

**Abbreviation:** ns, not significant.

## STV-Na Modulates the Plasma Metabolic Profiles in Colitis

STV-Na was further subjected to a plasma metabolite-based untargeted metabolomic study to discern the pharmacological mechanisms and likely pathogenesis of colitis. Metabolomics, a powerful systems biology approach, is used in evaluating medicines, discovering novel therapeutic agents, and monitoring treatment.<sup>37</sup> The metabolic impact and molecular mechanisms of drugs may be uncovered through the identification of various metabolites.<sup>38</sup>

This experiment utilized a metabolomic approach to study the metabolic responses of mice following DSS challenge and STV-Na treatment. OPLS-DA was used to investigate the differences between the DSS group and the treatment groups and between the control and DSS groups. In addition, PCA was used to determine the intrinsic similarity of the spectral profiles (Figure 3A and B). Each scatterplot displays a plasma sample in the positive-ion mode ( $R^2=88\%$ ) (Figure 3A) and negative-ion mode ( $R^2=89\%$ ) (Figure 3B). To assess the changes in metabolite abundances and to identify markedly varied metabolites, pairwise comparisons of the samples were conducted and analyzed by PLS-DA (Figure 3C and D). The PLS-DA plots obtained in this study fully segregated into an individual cluster, which illustrated that the plasma metabolic profiles showed marked changes among the groups. The PLS-DA plots obtained in the positive-ion mode, which exhibited an  $R^2$  of 95% and  $Q^2$  of 76% (Figure 3C), and the negative-ion mode, which exhibited an  $R^2$  of 95% and  $Q^2$  of 85% (Figure 3D) were capable of distinguishing each group.

These findings suggested the excellent discriminative performance of the model, with both control and DSS groups demonstrating metabolic phenotype separations. Control and STV-Na groups had more similar metabolic patterns in contrast to those of the DSS and control groups. Therefore, we revealed that the STV-Na and control groups exhibited similar metabolic phenotypes, which suggested that STV-Na treatment could prevent the DSS-triggered variations in plasma metabolites in mice with colitis.

The VIP and P values were then used to screen for potential variables likely causing group separation. The UpSet plot illustrated that the 10 overlapping metabolites were identified in the positive-ion mode (Figure 3E). A total of 13 metabolites overlapped in the negative-ion

mode (Figure 3F). Total metabolites found in each group are illustrated by the horizontal bars, whereas the vertical bars demonstrate intergroup intersections, shown in the matrix below the graph.

Volcano plots show the variables with contents that differ between groups (Figure 3G and H). The screened variables were identified using MS/MS fragmentation. Plasma analysis revealed 23 differentially accumulated metabolites (Supplementary Table 3 and Supplementary Figure 1). These metabolites comprised of glutaminyl-tryptophan, PIP3(18:1(11Z)/20:3(8Z,11Z,14Z)), OPC8-CoA, DL-homocystine, and PG(P-16:0/12:0), etc. A hierarchical clustering heatmap also suggested that these differentially accumulated metabolites were visibly differentiated between the control and DSS groups and were altered in the STV-Na groups (Figure 4A), which suggested that these metabolites were significant in IBDs after STV-Na treatment.

To explore the effect of STV-Na treatment on the IBD metabolic pathway, MetaboAnalyst 5.0 was used to carry out plasma analysis. Our data revealed the involvement of four major metabolic pathways: glycerophospholipid metabolism, riboflavin metabolism, porphyrin and chlorophyll metabolism, and phenylalanine metabolism (Figure 4B). Metabolites involved in these metabolic pathways were glycerophospholipids, riboflavin, porphyrin and chlorophyll, and phenylalanine. These metabolites were observably altered in the DSS group and adjusted following STV-Na treatment. These data demonstrated that STV-Na protected against IBDs by regulating metabolic reprogramming.

## STV-Na Regulates the Balance of M1/M2 Macrophage Polarization in Colitis

IBD development relies heavily on macrophage functions.<sup>7</sup> In an inflammatory state, macrophages secrete proinflammatory cytokines that result in tissue damage. M1 macrophages highly express TNF- $\alpha$  and IL-1 $\beta$ , which are associated with inflammation, chemotaxis, and the induction of matrix degradation. M2 macrophages exhibit anti-inflammation, tissue repair, and angiogenic properties. This study examined spleen and colon macrophage infiltration using by qPCR, flow cytometry, and immunofluorescence staining (Figure 5A). First, we evaluated the M1 macrophage mRNA expression profile in colonic tissue. We found that TNF- $\alpha$  and IL-1 $\beta$  expressions were significantly increased in the DSS group, which

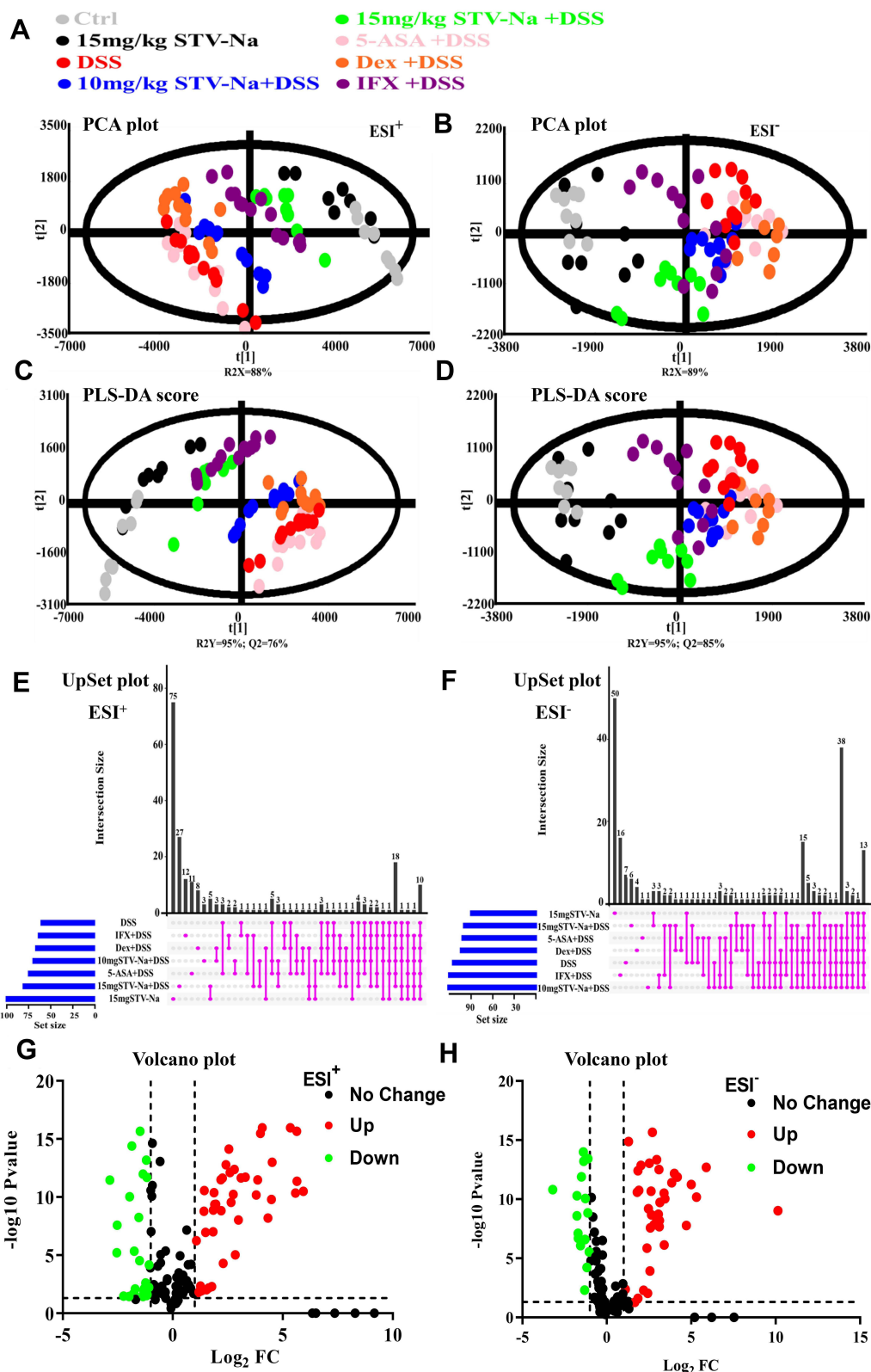


**Figure 3** An untargeted metabolomics study revealed that STV-Na could regulate the metabolic profiles in mice with colitis. (**A** and **B**) PCA score plots of plasma samples obtained from different groups in the ESI positive-ion mode (**A**) and negative-ion mode (**B**). (**C** and **D**) PLS-DA scores scatter plot. The discriminant models distinguished different groups in the ESI positive-ion mode (**C**) and ESI negative-ion mode (**D**). (**E** and **F**) UpSet plot showing the overlap of metabolites identified across each group in both the ESI positive-ion mode (**E**) and ESI negative-ion mode (**F**). The horizontal bars demonstrate total metabolites characterized in each group in both the ESI positive-ion mode (**E**) and ESI negative-ion mode (**F**). The vertical bars indicate intergroup intersections, as depicted in the matrix below the graph. (**G** and **H**) Volcano plot. A total of 144 and 138 variables were selected based on the fold change (>2) and P (<0.05) values in the ESI positive-ion mode (**G**) and ESI negative-ion mode (**H**) (n = 6 to 12 mice per group).

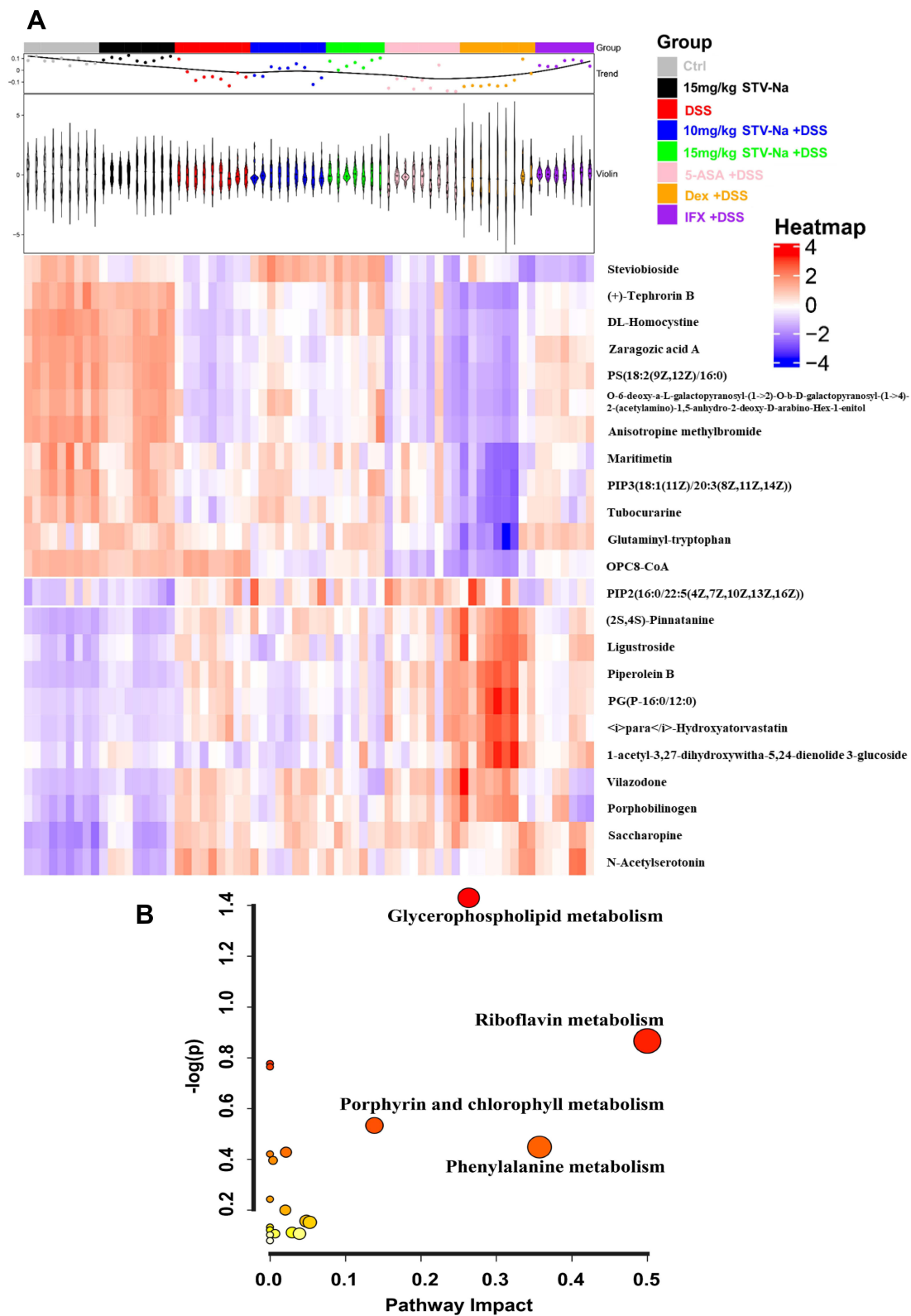


**Figure 4 (A)** Heatmap of differentially accumulated metabolites. Each metabolite is represented by a row and each sample is represented by a column. The red color represents high abundance, and blue indicates low abundance (n = 7 to 9 mice per group). **(B)** Metabolic pathway analysis of effects of STV-Na on colitis. Circle colors represent p values (y-axis) while circle sizes indicate the pathway impact (x-axis). The involved pathways of the circles are shown, with the red circles indicating pathways with significant changes.

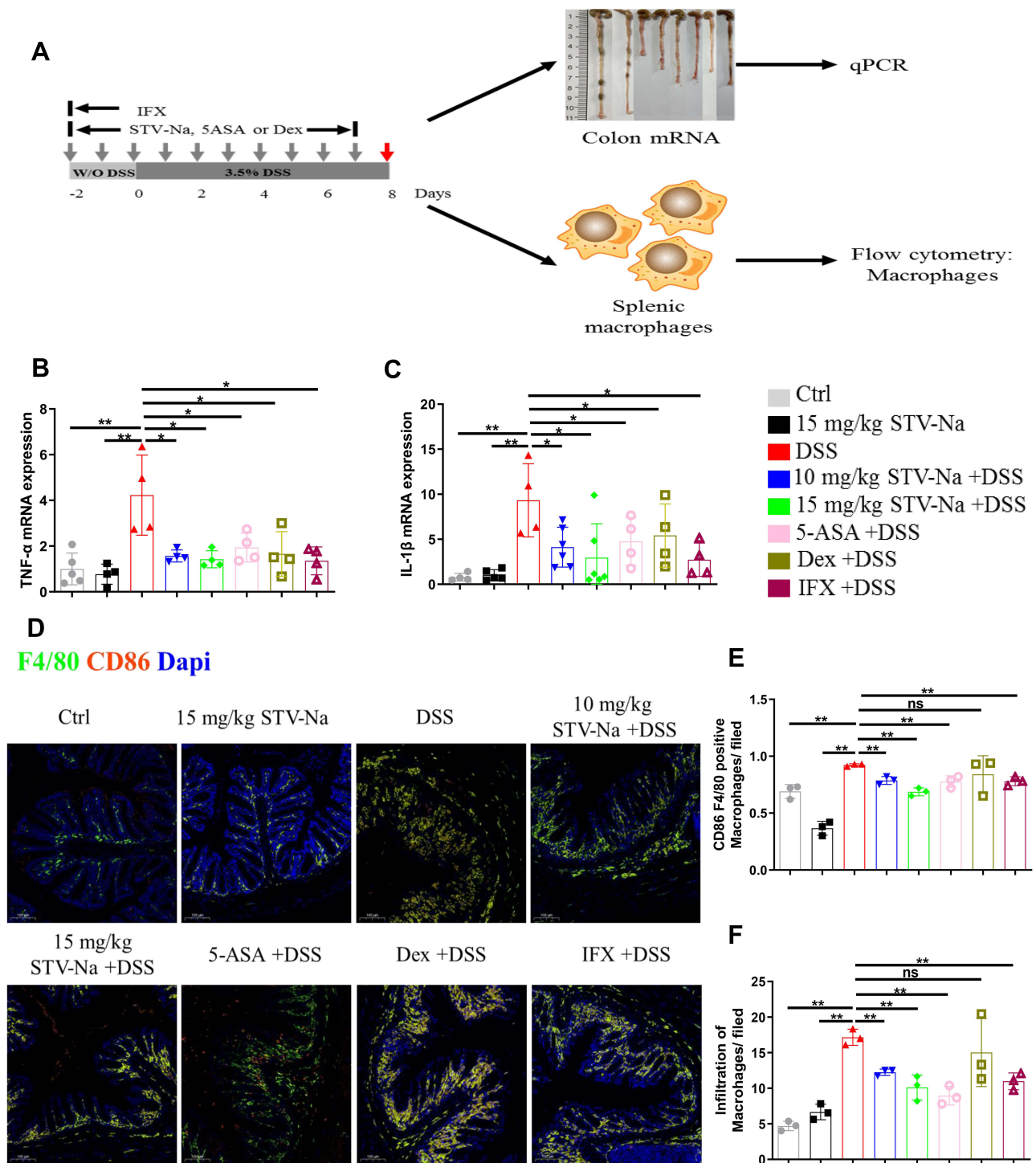


**Figure 5** STV-Na regulates the balance of M1/M2 macrophage polarization in mice with IBD. **(A)** Schematic of experiments analyzing macrophage polarization in DSS-triggered colitis. **(B and C)** TNF- $\alpha$  and IL-1 $\beta$  gene expression in colon tissues were examined by RT-qPCR. **(D)** Immunofluorescence staining (scale bars: 100  $\mu$ m) of F4/80+ and F4/80+CD86+ macrophages in colonic tissues from mice with DSS-induced colitis. **(E and F)** Quantification of M1 (CD86+F4/80+) **(E)** and M0 (F4/80+) **(F)** macrophages per field. Data are published in terms of means  $\pm$  SDs. The statistical analyses were performed with Student's t-test or one-way ANOVA followed Turkey's post hoc test (n = 3 to 6 mice per group; each data point represents one mouse); \*P < 0.05 and \*\*P < 0.01 in contrast to the DSS group. **Abbreviation:** ns, not significant.

corroborated with the finding that DSS challenge induces macrophage polarization. In contrast, mRNA expressions of TNF- $\alpha$  and IL-1 $\beta$  were reduced in the STV-Na-,

5-ASA-, Dex-, and IFX-treated groups (Figure 5B and C). In addition, an immunofluorescence analysis of colon tissue using F4/80 (marker of macrophages including M0

macrophages) and CD86 (marker of M1 macrophages) demonstrated that STV-Na, 5-ASA and IFX significantly inhibited both M0 and M1 macrophages in the colons of mice with DSS-induced colitis (Figure 5D–F and Supplementary Figure 3). In the present study, Dex treatment did not significantly inhibit M0 and M1 macrophages. Furthermore, colonic specimens of each group did not demonstrate marked variability in the M2 macrophage population or in CD163 expression (Supplementary Figures 2 and 3).

This phenomenon was also demonstrated using flow cytometry analysis (Figure 6). A previous study has shown that DSS-induced colitis increased the spleen index of mice,<sup>35</sup> which is in line with our findings. To investigate the effects of STV-Na on macrophage polarization in the spleens of mice with DSS-triggered

colitis, a flow cytometric analysis was performed which revealed a higher ratio and absolute cell numbers of M0 (F4/80+CD11c-CD206-), M1 (F4/80+CD11c+CD206-), and M2 (F4/80+CD11c-CD206+) macrophages in the DSS group in contrast to the control group. In addition, STV-Na or IFX treatment reduced the ratio and absolute cell numbers of M0, M1, and M2 macrophages in mice with colitis in contrast to those of the DSS cohort (Figure 6A and B and Supplementary Figure 4). Interestingly, 5-ASA inhibited M1, but not M2 macrophage polarization, while Dex failed to inhibit either of these processes. These results suggested that STV-Na resolved colonic inflammation in part by balancing the degree of M1 and M2 macrophage polarization, thereby promoting recovery of the injured colon.

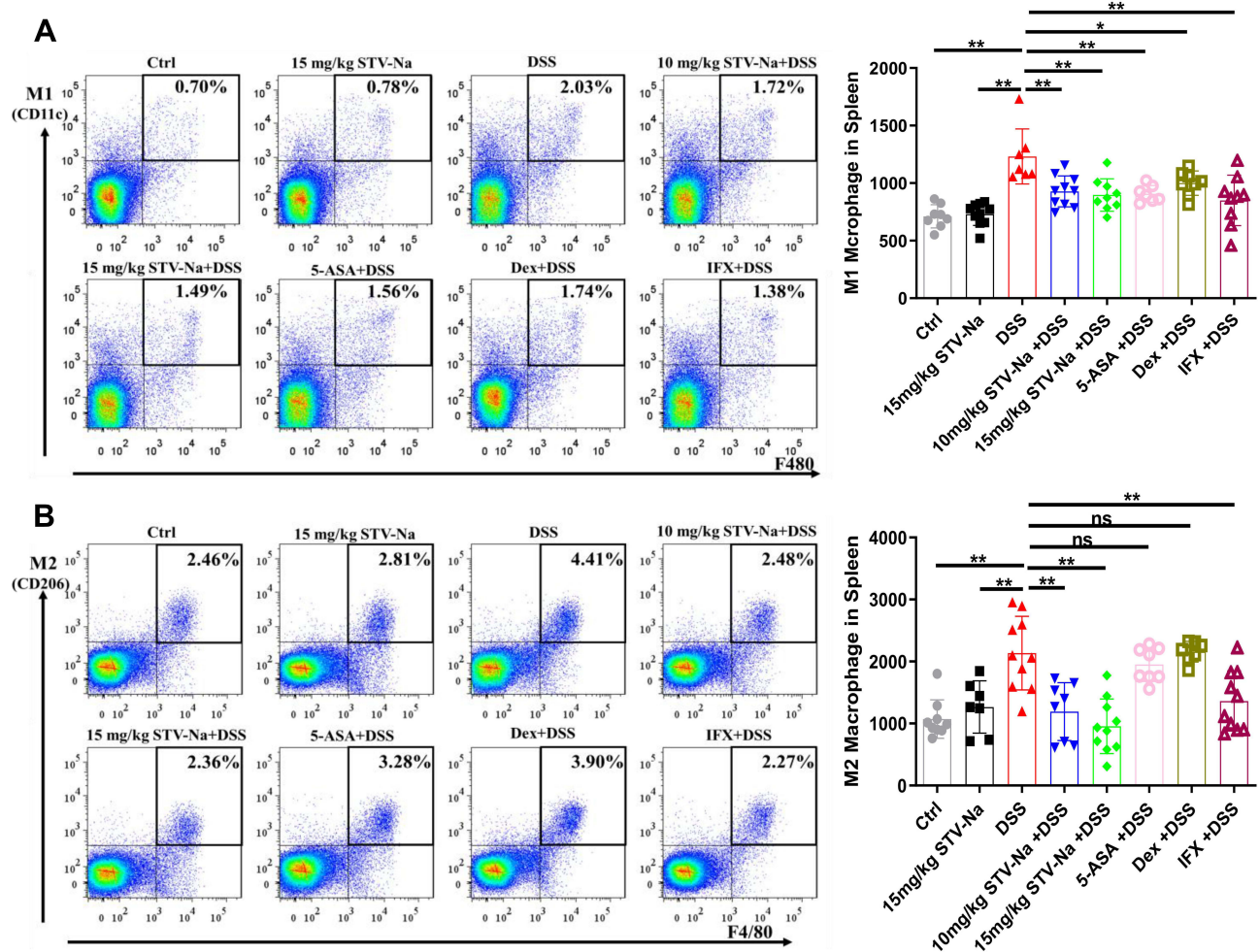


**Figure 6** STV-Na restores the balance of M1/M2 macrophage polarization in the spleens of mice with IBDs. (A and B) The percentages and absolute numbers of M1 macrophages (F4/80+CD11c+CD206-) (A) and M2 macrophages (F4/80+CD11c-CD206+) (B) in the spleen were analyzed by flow cytometry. Data are published in terms of means  $\pm$  SDs. The statistical analyses were performed with Student's *t*-test or one-way ANOVA followed Turkey's post hoc test ( $n = 6$  to 12 mice per group; each data point represents one mouse); \* $P < 0.05$  and \*\* $P < 0.01$  in contrast to the DSS group. **Abbreviation:** ns, not significant.

## STV-Na Restores the Balance of Treg, Th17, Th2, and Th1 Cells in Mice with DSS-Induced Colitis

In addition to macrophages, CD4<sup>+</sup> Th cells play a pivotal role in the pathogenesis of IBDs.<sup>6</sup> IBDs are associated with a distinct populations pattern of Th cells. Previous studies have observed raised Th1 and Th2 cell numbers in the injured intestinal lamina propria of IBD patients, with Th17 and Treg cells specifically found to be related to IBDs.<sup>39</sup> Therefore, we sought to characterize the general Th cell population and identify distinct populations of Th cells in the colons and spleens of our mice models. To elucidate the underlying mechanism through which STV-Na ameliorates colitis, the effects of STV-Na treatment on T cell activation and the induction of regulatory T cells were evaluated using colons of mice with colitis. We first examined the mRNA expression levels of Th1 cells (IFN- $\gamma$ ), Th2 cells (IL-4), and Th17 cells (IL-17A) in colon tissues by qPCR. Our results revealed that DSS challenge increased the mRNA levels of IL-17A, IL-4, and IFN- $\gamma$  by 7.52-, 2.70-, and 3.09-fold, respectively, in contrast to those of the control group (Figure 7A). The STV-Na, 5-ASA, Dex, and IFX groups demonstrated suppressed mRNA expression levels of IFN- $\gamma$ , IL-4, and IL-17A in the colon in comparison to the DSS group.

Furthermore, the general splenic T cell population was characterized using a combination of CD3 and CD4 markers. We isolated splenocytes from each group and phenotyped these cells using flow cytometry. The general T cell population was notably suppressed in DSS-induced mice, whereas STV-Na and 5-ASA treatment significantly increased the number of T cells. Treatment with Dex or IFX trended toward a higher T cell population in contrast to those of the DSS group (Supplementary Figure 5).

We then performed intracellular/intranuclear staining to identify the effect of STV-Na on specific CD4<sup>+</sup> T cell subsets, such as the Treg (CD4<sup>+</sup>CD25<sup>+</sup>Foxp3<sup>+</sup>) cells, Th17 (CD4<sup>+</sup>IL-17A<sup>+</sup>) cells, Th2 (CD4<sup>+</sup>IL-10<sup>+</sup>) cells, and Th1 (CD4<sup>+</sup>IFN- $\gamma$ <sup>+</sup>) cells. Our data showed significant decreases in both the percentage and absolute counts of Th1, Th2, and Th17 cells in the STV-Na treatment group compared with the DSS group. Interestingly, these suppressive effects of STV-Na were similar to those of 5-ASA, Dex, and IFX (Figure 7B–D). Our findings are in line with the results of colonic tissue RT-qPCR analysis of the colon (Figure 7A). In contrast, intranuclear staining for Tregs, which usually suppress inflammation, showed

significant decreases in both their percentage and absolute cell number in the DSS groups, STV-Na or Dex groups but not the 5-ASA or IFX group reversed this effect (Figure 7E).

Collectively, these data showed that STV-Na treatment could regulate the balance of Th1, Th2, Th17, and Tregs in DSS induced IBD mice by reducing the Th1, Th2, and Th17 cell responses and promoting the production of specific T cell subsets, mainly Treg-producing CD3<sup>+</sup>CD4<sup>+</sup> cells. Overall, these findings indicated that STV-Na exerted protective effects when used for IBDs treatment, with these effects partly mediated through maintenance of the Th1/Th2/Th17/Treg balance.

## STV-Na Ameliorates DSS-Induced Damage to the Intestinal Barrier by Restoring the Functions of Tight Junctions

The selectively permeable intestinal barrier protects enterocytes against external threats such as toxins, antigens, and pathogenic microorganisms. DAO is a cytoplasmic enzyme that is present in mammalian mucosa and is abundantly found in the intestinal mucosa, but rarely in serum. Cytoplasmic DAO is released systemically through the bloodstream upon intestinal mucosal epithelial damage.<sup>40</sup> The impact of STV-Na on intestinal epithelial permeability was investigated using an *in vivo* permeability assay with FITC-dextran was performed. STV-Na treatment resulted in notably less permeable intestinal barriers compared to that observed in DSS-treated groups (Figure 8A). Furthermore, LPS and DAO serum were notably elevated in the DSS group in contrast to the control group, suggesting that DSS made the intestinal barrier more permeable. However, STV-Na significantly decreased the levels of LPS and DAO by 53.02% and 48.20%, respectively, in contrast to those seen in the DSS group (Figure 8B and C).

AB-PAS staining was conducted to examine the intestinal crypt morphology and the population of mucin-filled goblet cells upon drug treatment. DSS treatment resulted in a loss of goblet cells in contrast to the control group, a finding that was reversed with STV-Na exposure. Similarly, DSS caused reduced crypt depths while STV-Na again reversed this finding (Figure 8D–F).

STV-Na, 5-ASA, and IFX treatments were protective against goblet cell loss (Figure 1H). Regenerating islet-derived 3 $\gamma$  (Reg3 $\gamma$ ), an antimicrobial peptide, is associated with pathological injury and inflammation levels. Goblet cells produce MUC2 which critically contributes towards

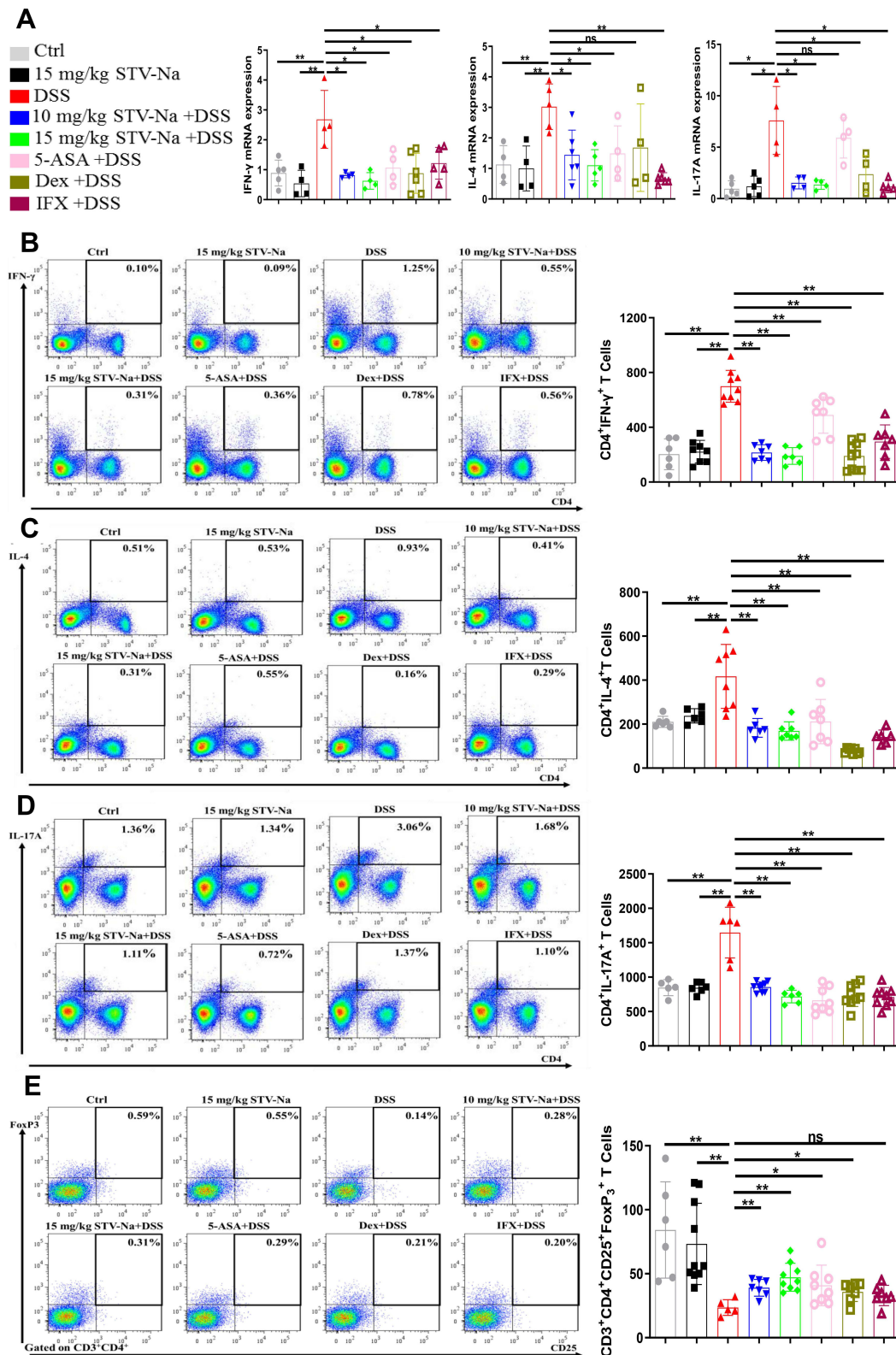


**Figure 7** STV-Na restores the balance of Th1 cells, Th2 cells, Th17 cells, and Tregs by enhancing the production of Tregs in mice with IBDs. Mice with DSS-triggered acute colitis were administered either saline, STV-Na, 5-ASA, Dex, or IFX. **(A)** IFN- $\gamma$ , IL-4, and IL-17A gene expression in colon tissues was examined by real-time qPCR. **(B–E)** The percentages and absolute numbers of Th1 (CD4+IFN- $\gamma$ +), Th2 (CD4+IL-10+), Th17 (CD4+IL-17A+), and Treg (CD25+Foxp3+) cells in the spleen were analyzed by flow cytometry. Data are published in terms of means  $\pm$  SDs. The statistical analyses were performed with Student's *t*-test or one-way ANOVA followed Turkey's post hoc test (*n* = 4 to 12 mice per group; each data point represents one mouse); \**P* < 0.05 and \*\**P* < 0.01 in contrast to the DSS group. **Abbreviation:** ns, not significant.

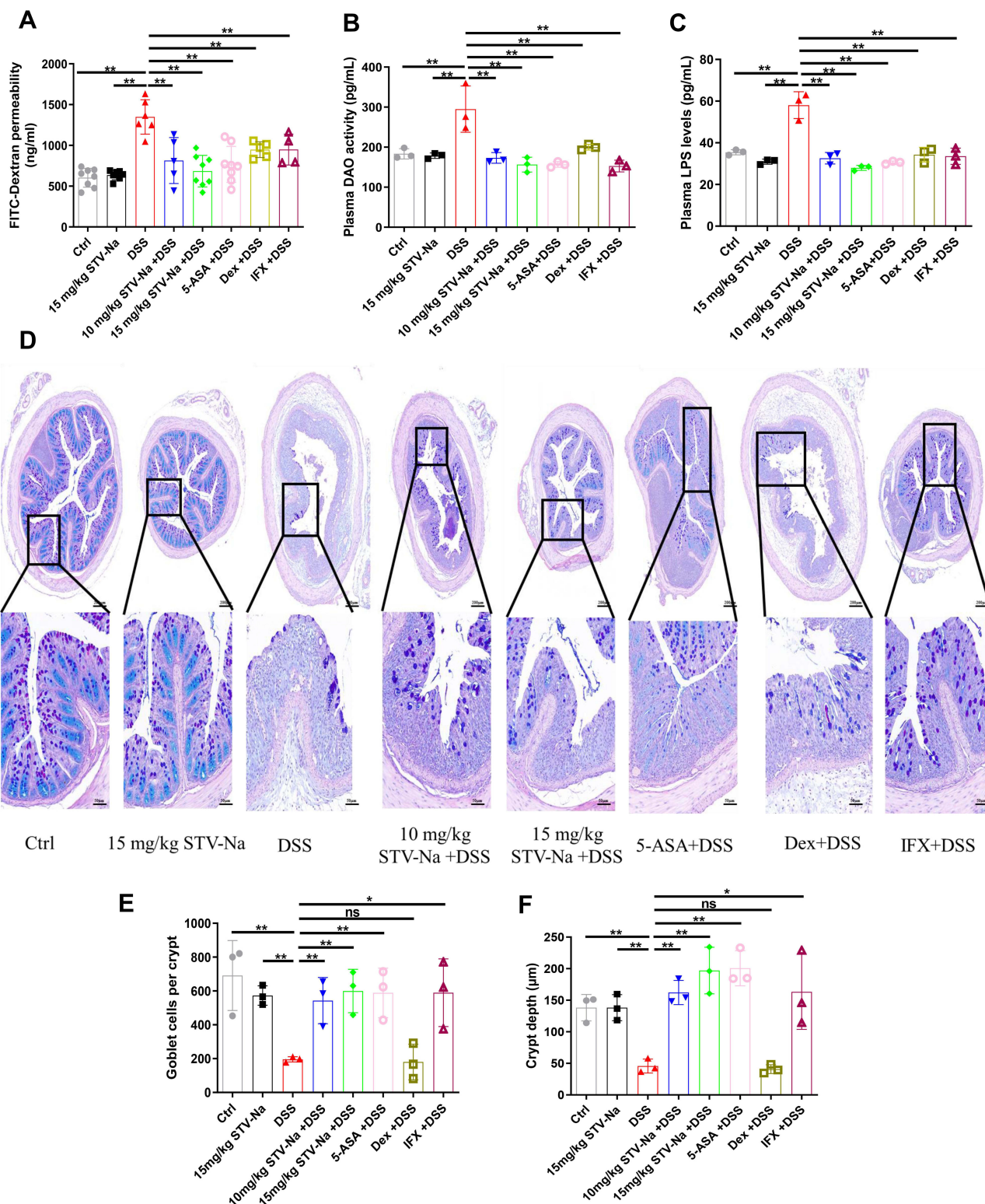


**Figure 8** STV-Na improves intestinal permeability in mice with IBDs. **(A)** Intestinal permeability was analyzed via the intragastric administration of 4.0-kDa FITC-dextran. **(B)** DAO activity in plasma. **(C)** Endotoxin (LPS) levels in plasma. **(D)** Typical histological images of AB/PAS-stained colonic tissue from different groups. Scale bars, 200 µm (50 µm in the magnified images). **(E)** Number of goblet cells. **(F)** The crypt depth in each group was assessed. Data are published in terms of means ± SDs. The statistical analyses were performed with Student's *t*-test or one-way ANOVA followed Turkey's post hoc test (*n* = 3 to 8 mice per group; each data point represents one mouse); \**P* < 0.05 and \*\**P* < 0.01 in contrast to the DSS group.

**Abbreviation:** ns, not significant.

intestinal barrier function as it represents a principal molecule in intestinal mucus.

In contrast to the control group, DSS exposure showed remarkably increased mRNA expression of Reg3 $\gamma$  and decreased mRNA expression of MUC2. Conversely, STV-Na, 5-ASA, Dex, and IFX significantly downregulated the expression of Reg3 $\gamma$  (Figure 9A). The DSS group showed reduced MUC2 mRNA and protein expressions in colon tissue in contrast to the control group (Figure 9B, F, and G), while STV-Na, 5-ASA, Dex, and IFX significantly upregulated the mRNA and protein expressions of MUC2 (Figure 9B, F, and G). STV-Na treatment restored the lost MUC2 expression (Figure 9F and G), indicating that STV-Na could maintain the epithelial barrier by protecting the mucus layer and restricting goblet cells.

Epithelial integrity is maintained by epithelial tight junctions, which critically protect against inflammation. Therefore, STV-Na effects on colonic tight junction proteins mRNA expression, including ZO-1, claudin-1, and occludin were evaluated by RT-qPCR and immunohistochemical analysis. As depicted in Figure 9C, D, and E, the mRNA expressions levels of ZO-1, claudin-1, and occludin were markedly downregulated in the DSS group. In addition, STV-Na treatment significantly restored the mRNA expression of ZO-1 and claudin-1. Immunohistochemical evaluation revealed widely distributed ZO-1 and claudin-1 across the superficial layer of the lamina and epithelium in the control group (Figure 9F, H, and I).

Likewise, there were notably suppressed claudin-1 and ZO-1 mRNA and protein levels seen in the DSS group. STV-Na exposure maintained epithelial cell expressions of these molecules at the baseline levels. Thus, these findings demonstrated that STV-Na might render the colonic epithelium less permeable by protecting TJs.

## Discussion

This series of experiments explores the effects and underlying mechanisms of STV-Na treatment in IBDs by utilizing a DSS-stimulated IBD mouse model. The findings obtained in this study demonstrate that STV-Na confers a therapeutic effect on colitis through inhibition of macrophage infiltration and polarizing macrophage phenotypes, regulating the Th1/Th2/Th17/Treg balance, metabolic programming, and maintaining epithelial integrity. We conclude that these findings underscore the therapeutic potential of STV-Na for preventing and treating IBDs by

modulating the immune response and metabolic reprogramming.

The pathogenesis of IBDs remains unclear. Mounting evidence suggests that the etiology of IBDs may be associated with an excessive immune response and various metabolic dysregulations.<sup>4,5</sup> Current therapeutic drugs against IBDs exhibit limited efficacy, unsatisfactory clinical outcomes, and severe side effects, while incurring high costs, all of which further limit the clinical application of these drugs.<sup>13,15</sup> Some studies also found that terpenoids and anti-oxidants can relieve the intestinal inflammation of IBDs.<sup>41-43</sup> In the present work, three drugs, commonly prescribed for the management of IBDs which included 5-ASA, Dex, and IFX, were used as positive controls to assess the efficacy of STV-Na. In the present study, we found that the efficiency of STV-Na was equal to or even greater than that of 5-ASA and Dex. More benefits were seen at high doses of STV-Na at a high dose (STV-Na, 15 mg/kg) for treating experimental IBDs.

IBDs are characterized by body weight loss, bloody feces, diarrhea, shortening of the colon length, and splenomegaly.<sup>1</sup> We found significant reductions in body weight and colon length, along with increases in the spleen index following DSS exposure. STV-Na was able to alleviate these symptoms. Additionally, STV-Na induced a noticeable decline in microscopic epithelium disruption and decreased the levels of WBCs, NEUTs, LYMPHs, and MONOs. These findings further confirm and provide evidence that STV-Na exerts a protective effect on DSS induced IBDs and may have clinical utility in treating of IBDs.

A previous study suggested results in severe gastrointestinal tract bleeding, RBC hemolysis, and poor intestinal iron absorption. Both children and adults with IBDs commonly exhibit anemia.<sup>44</sup> RBCs, HGB, and HCT are usually lower in patients with IBDs than in healthy individuals. A decrease in RBCs reveals an imbalance between the production and loss of RBC's.<sup>45</sup> Our data demonstrated that DSS-stimulated colitis yielded markedly reduced RBCs and HGB levels. STV-Na administered at the doses used in this study and for the duration of the experiment appeared to improve the RBC and HGB counts in contrast to those found in the control group. Based on these data, we revealed that STV-Na completely inhibited the effect of DSS on colonic blood loss.

An increasing number of research have revealed that IBDs harbor a proinflammatory profile comprising of

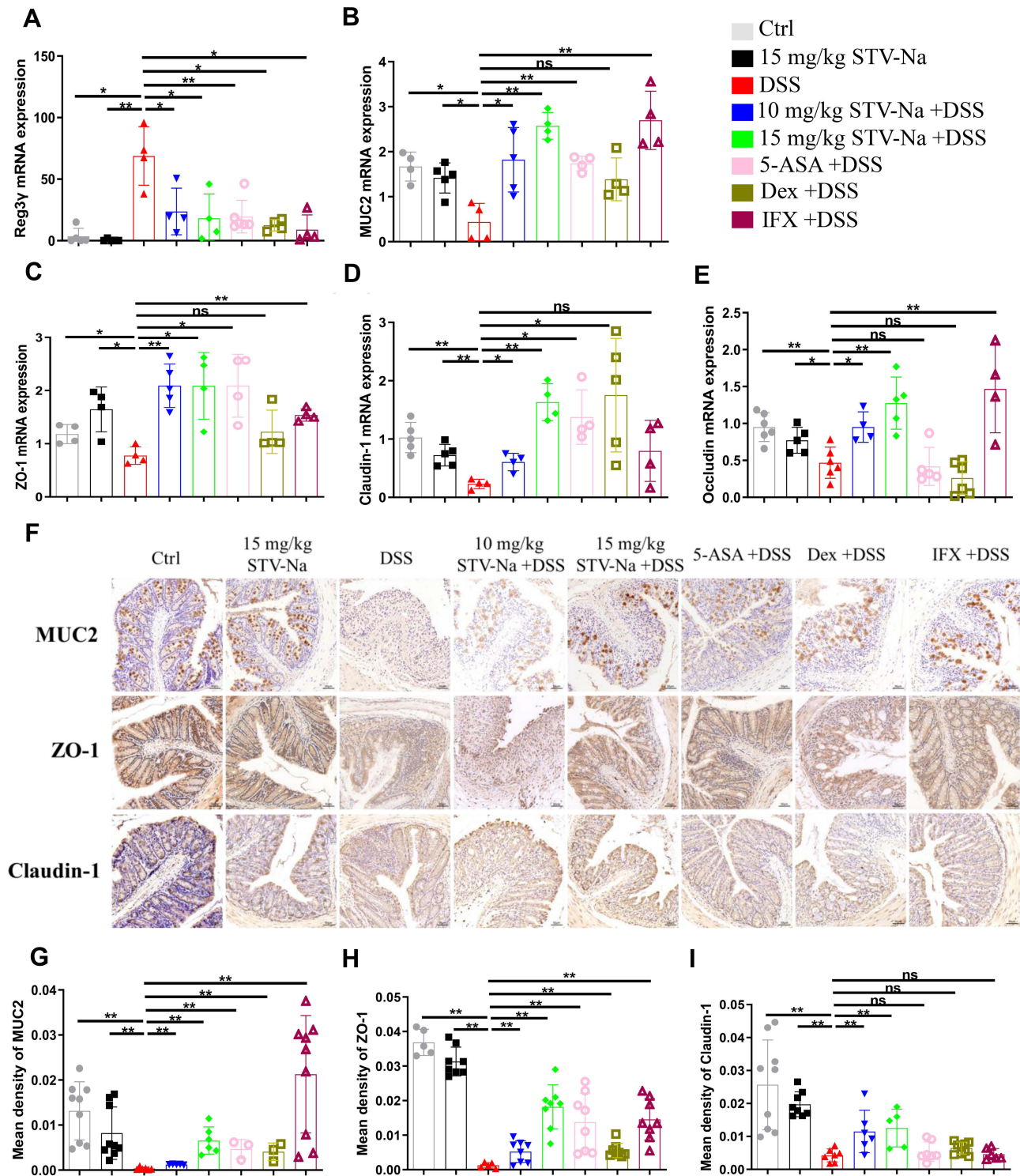


**Figure 9** STV-Na ameliorates DSS-induced damage to the intestinal barrier through the restoration of tight junction function. (A–E) The mRNA levels of colonic Reg3 $\gamma$  (A), MUC2 (B), ZO-1 (C), Claudin-1 (D), and Occludin (E) were examined by RT-qPCR. (F) The distribution of MUC2, ZO-1, and Claudin-1 in colonic tissues was evaluated by immunohistochemical staining. (G–I) Quantification of the immunohistochemical intensity reflecting the expression of MUC2 (G), ZO-1 (H), and claudin-1 (I) in the mice colon. Data are published in terms of means  $\pm$  SDs. The statistical analyses were performed with Student's *t*-test or one-way ANOVA followed Turkey's post hoc test (*n* = 4 to 10 mice per group; each data point represents one mouse); \**P* < 0.05 and \*\**P* < 0.01 in contrast to the DSS group.

**Abbreviation:** ns, not significant.

increased IL-1 $\beta$ , IFN- $\gamma$ , IL-2, TNF- $\alpha$ , and IL-18 levels, which are speculated to be vital initiating and perpetuating agents of intestinal inflammation.<sup>6</sup> The early phase of inflammation is triggered by IFN- $\gamma$  and IL-1 $\beta$ .<sup>46</sup> TNF- $\alpha$  perpetuates an inflammatory cycle by stimulating cytokine release from T cells and macrophages, which results in altered intestinal barrier function and causes intestinal epithelial cell apoptosis.<sup>47</sup> IL-18 is a crucial epithelial-derived cytokine regulating distinct subsets of intestinal CD4+ T cells in proinflammatory microenvironments. Additionally, nuclear factor (NF)- $\kappa$ B is involved in the regulation of IL-18 and IL-1 $\beta$  gene expression.<sup>12</sup>

IL-2 expression is induced by IL-1 $\beta$ , thereby accelerating inflammation.<sup>48</sup> Furthermore, IL-18 stimulates IFN- $\gamma$  release while augmenting Th1 cell proliferation that goes on to modify the inflammatory response.<sup>49</sup> Moreover, colitis-associated anemia occurs as a result of raised inflammatory cytokines such as TNF- $\alpha$  and IL-1 $\beta$ . IL-1 $\beta$  negatively regulates the absorption and release of iron while the amount of iron is reduced by TNF- $\alpha$ -instigated elevations in ferritin production. Patients with IBDs are iron-deficient,<sup>45</sup> and iron deficiency exerts subtle effects on the immune function as it is involved in ferroptosis.<sup>50</sup> Several studies have shown that ferroptosis is an essential contributor to the development of IBDs.<sup>51</sup> The current study shows that mice with colitis with initially elevated levels of IL-1 $\beta$ , IFN- $\gamma$ , IL-2, TNF- $\alpha$ , and IL-18 had these cytokines suppressed upon STV-Na treatment, an occurrence that directly attributed to the inhibition of NF- $\kappa$ B activation. Our previous studies have shown that STV-Na can inhibit NF- $\kappa$ B in diabetic cardiomyopathy in rats.<sup>22</sup> More in-depth investigations looking into the potential interactions between STV-Na and NF- $\kappa$ B in IBDs are warranted. In addition, colitis-associated anemia may also occur as a result of this pathway due to inflammation causing iron deficiency. These findings are in line with the hematological results and suggest that STV-Na may ameliorate the pathology by regulating immune-associated cytokines. Further research is needed to determine whether STV-Na is involved in ferroptosis-mediated inhibition of IBDs.

Recent studies have shown that altered metabolite levels may potentially function as a biological indicator of gut health.<sup>5</sup> The production of specific metabolites highlights ongoing inflammation and activated immune cells. Inflammation induces macrophages, neutrophils, and Th cell aggregation while promoting lipid oxidation and the production of inflammatory cytokines.<sup>52</sup>

Therefore, high levels of lipid oxidation and excessive inflammatory cytokine levels indicate inflammatory cell infiltration. Intraperitoneal administration of STV-Na reversed the effects of colitis on metabolites involved in lipid oxidation and inflammation, and the levels obtained with this treatment reflected those obtained in the control group. Thus, we hypothesize that these metabolites may play an indispensable role in IBDs. Our analysis revealed several metabolic pathways that significantly differed after treatment. Lipid metabolism is critically modulated by glycerophospholipid metabolism. This pathway is constantly stimulated during inflammation and in response to oxidative stress, which might alter the expressions of the immune-related cytokines IFN- $\gamma$  and IL-2,<sup>53</sup> in agreement with our study. However, the effect of STV-Na on oxidative stress requires further exploration, and more in-depth investigations are needed in this area. Phenylalanine is an endogenous energy-promoting neuroamine regulating physiological stress that has been linked to inflammation.<sup>54</sup> Stress-induced increase in energy metabolism could likely be behind the metabolic profile changes in our IBD mice models, in order to account for additional energy demand due to inflammation. Yu et al reported similar findings<sup>55</sup> and found that IBD is associated to changes in lipid metabolism and energy metabolic intermediates that occur to match the metabolic demands of intestinal inflammation. Hemoglobin is dependent on chlorophyll and porphyrin metabolisms,<sup>56</sup> while riboflavin metabolism may be related to the production of inflammatory cytokines in IBDs.<sup>57</sup> STV-Na administration significantly changed these metabolic pathways by inhibiting inflammation. However, the relationship between immune cells like Th cells and macrophages and metabolism requires further experimental verification. A comprehensive analysis consisting of hematological evaluation, cytokine microarray assay, and untargeted metabolomics suggested that the immune response is the dominant mechanism through which STV-Na protects against colitis.

IBD severity and incidence are closely linked to the profile and extent of immunological activation.<sup>1</sup> Macrophage populations are more prominent in patients with active IBDs compared to in healthy donors.<sup>7</sup> Th (Th1/Th2/Th17/Treg) cells are pivotal in maintaining inflammatory homeostasis in both diseased and healthy conditions. Depleted T cell and macrophage populations prior to the onset of DSS-induced colitis cause disease exacerbations.<sup>11</sup> The current experiments observed the impact of STV-Na on splenic and colonic macrophages

and Th cells in DSS-induced IBDs mice, and STV-Na treatment attenuated the increases in macrophages, and restored the Th1/Th2 and Treg/Th17 cell balance.

Immune responses are mediated by macrophages activation, which act as immune system sentinels in peripheral tissue sentinels. A proinflammatory state is mediated by M1 macrophages while tissue repair and inflammation resolution are mediated by M2 macrophages. A dysregulated balance between these two polarized states results in inflammatory injury and IBD repair.<sup>7</sup> We sought to determine whether STV-Na could abolish the inflammatory response in IBD by regulating macrophage polarization.

As expected, STV-Na-treated mice showed down-regulated mRNA expression of M1-related cytokines TNF- $\alpha$  and IL-1 $\beta$  in contrast to the DSS group mice. Additional investigations found that the primary cells responsible for synthesizing and releasing inflammatory factors are M1 macrophages.<sup>8</sup> STV-Na treatment promoted anti-inflammatory activity by suppressing M1 macrophage polarization in spleen and colon tissue and releasing inflammatory factors in mice with DSS-induced IBD, which resulted in a reduction in intestinal injury. In animal models of ischemic stroke, STV-Na has also been demonstrated to attenuate neuroinflammation by suppressing M1 microglia/macrophage responses.<sup>30</sup> STV-Na also exerts a protective effect against diabetic cardiomyopathy in rats by inhibiting cardiac inflammation.<sup>22</sup> We therefore postulate that the anti-inflammatory effects of STV-Na may be linked to suppression of M1 macrophage polarization. Similarly, STV-Na suppressive effects on M2 macrophage polarization, as seen by a decreased M2 proportion. The induction of a higher number of M2 macrophage in IBD patients may be an essential mechanism resulting from the induction of matrix deposition and fibrosis.<sup>58</sup> However, future studies are needed to clarify whether STV-Na inhibits M2 polarization through proliferation and induction of matrix deposition. These observations suggest that STV-Na suppresses the inflammatory response by inhibiting M1 and M2 macrophage polarization rather than shifting M1 to M2 macrophages. These findings are also in line with previous studies on STV-Na.

Besides macrophage activation, disrupted Th17/Treg and Th1/Th2 homeostasis also brings about uncontrolled inflammation that culminates in progressive mucosal damage and disease propagation given the unrestrained production of inflammatory factors such as IL-17 and IFN- $\gamma$ .<sup>59</sup> Herein, we found that STV-Na treatment

sufficiently normalized splenic Th17/Treg and Th1/Th2 balances in a DSS-induced IBD mice model, while simultaneously suppressing the mRNA expression of IFN- $\gamma$ , IL-4, and IL-17A. Additionally, our results reflect those of previous studies that noted decreased T cell percentages and reduced CD4+ T cell counts in iron deficiency.<sup>50</sup> However, STV-Na administration decreased IL-4 secretion, although there was also a decrease in the number of Th2 cells, which we attribute to the dual role of IL-4 in colitis. The progression from acute to chronic inflammation is accompanied by a shift from primarily Th1/Th17-mediated immune responses toward one that predominantly features Th2-mediated inflammatory responses, which in turn is marked by raised IL-4 and decreased IL-17 levels.<sup>59</sup>

Previous investigations have found that IL-33 mediated exacerbations of acute colitis are reliant on IL-4 expression.<sup>60</sup> STV-Na exposure triggers a complex cascade that regulates the initiation and persistence of inflammation. In any case, IFN- $\gamma$  and IL-4 have been demonstrated to exert antagonistic effects on Treg cell conversion during inflammation.<sup>61</sup> Therefore, the STV-Na administration-induced increase in Treg cells may also negatively regulate IL-4 production. Interpreted as a whole, STV-Na appears to be effective in controlling the Th1/Th2 and Th17/Treg cell balance in maintaining immune homeostasis. Normalizing the relative frequencies of Th1/Th2/Th17/Treg cells might serve as an efficacious means of alleviating IBD-associated morbidity. However, the potential mechanisms through which macrophages interact with T cells have not yet been fully explored, and more in-depth investigations are needed in this area.

TJs are well-known components contributing to intestinal integrity and dysfunction and are highly associated with metabolic and inflammatory diseases.<sup>1</sup> The disruption of TJs is involved in IBD development by allowing the translocation of macromolecules, endotoxins, and bacteria. Consistent with data from patients with IBDs,<sup>62</sup> DSS-triggered colitis caused disrupted ZO-1, claudin-1, and occludin TJs. We also found that STV-Na prevented the DSS-induced disruption of TJs. This phenomenon agrees with other studies that showed increased occludin expression in glucose and oxygen-deprived murine brain capillary cerebellar endothelial cells.<sup>63</sup> In addition, STV-Na made the intestinal barrier less permeable by inhibiting the DSS-induced increases in FITC-dextran, endotoxin and DAO levels. Cerebral ischemia-induced injury appears

to be alleviated upon exposure to STV-Na.<sup>23,30</sup> Based on the present data, whether the protective effects of STV-Na are mediated through central mechanisms is unclear. Neuroprotective agents that act via the brain-gut axis have been proposed for the treatment of patients with IBDs.<sup>64</sup> It appears that this underrecognized pathway may be central in the protective effects of STV-Na in IBDs, although further study is needed. Moreover, the expression of mucus layer protecting proteins (MUC2) and antimicrobial proteins (Reg3 $\gamma$ ), the number and size of goblet cells and the crypt depth were significantly increased after STV-Na treatment, which indicated that STV-Na promoted goblet cell function and inner mucus layer production. These results suggest that STV-Na restores the intestinal barrier integrity and mucosal homeostasis and relieves colon damage.

In summary, this series of experiments sought to reveal the therapeutic effect of STV-Na against DSS-induced murine experimental colitis. STV-Na may potentially mediate this positive effect by regulating the immune response and metabolic reprogramming.

This study showed that STV-Na exerted an appreciable anti-colitic effect in the treatment of murine experimental UC induced by DSS. Our present study provides a foundation and justification for future research. STV-Na is a potential complementary therapeutic agent that can be combined with or used as an alternative to currently available drugs.

## Conclusion

Our study uncovers novel insights into the anti-colitic effects of STV-Na against DSS-induced mice models of colitis. STV-Na likely exerts its positive effects by regulating the immune response, reprogramming the metabolic profile associated with the regulation of the immune response and metabolic reprogramming, maintenance of the integrity of the intestinal barrier, and subsequent down-regulation of inflammatory mediators (Figure 10). Our investigation provides experimental evidence for the pharmaceutical application of STV-Na as a promising candidate in the treatment of IBDs and opens up a possible clinical application of STV-Na.

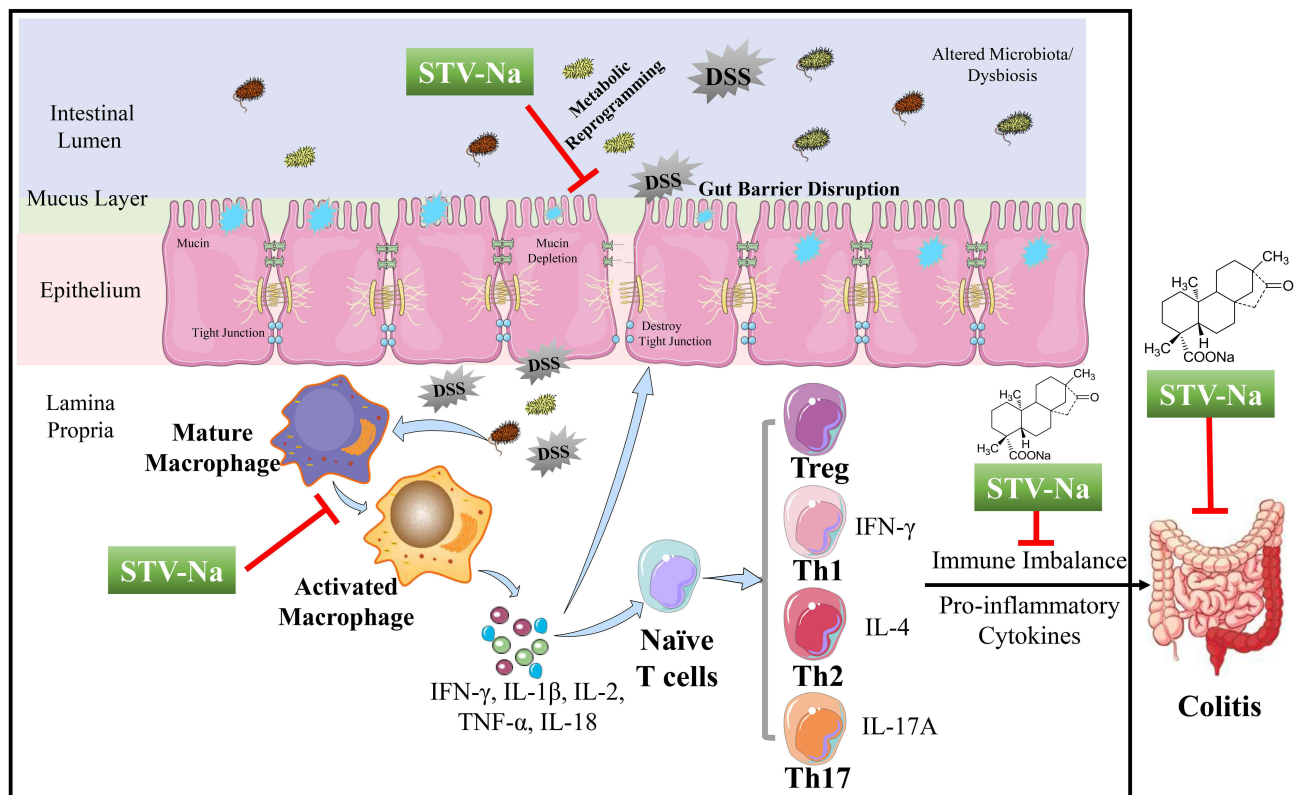


**Figure 10** Proposed mechanism through which STV-Na suppresses DSS-triggered IBD in mice. In the pathogenesis of colitis, a dysregulated immune response (macrophage polarization and Th1/Th2/Th17/Tre cells imbalance) accounts for the abnormal metabolism. Cytokine expression levels were significantly altered in DSS-induced mice compared with healthy controls, and this alteration led towards disrupted intestinal barrier integrity in mice. The treatment of DSS-induced mice with STV-Na resulted in marked improvements in dysregulated metabolic profiles, primarily glycerophospholipid, riboflavin, porphyrin and chlorophyll, and phenylalanine metabolism. STV-Na further improved the immune response and intestinal barrier dysregulation by reconstituting the gut barrier integrity in mice with DSS-induced IBDs.

## Abbreviations

IBDs, inflammatory bowel diseases; UC, ulcerative colitis; CD, Crohn's disease; STV-Na, isosteviol sodium; DSS, dextran sodium sulfate; 5-ASA, 5-aminosalicylic acid; Dex, dexamethasone; IFX, infliximab; LPS, lipopolysaccharides; DAO, diamine oxidase; TJ, tight junction; AB/PAS, Alcian blue/periodic acid-Schiff; UHPLC-TIMS-TOF-MS/MS, ultra-high performance liquid chromatography combined with trapped ion mobility spectrometry coupled to time-of-flight tandem mass spectrometry; FITC, fluorescein isothiocyanate; BV, brilliant violet; PE, phycoerythrin; WBC, white blood cell; NEUT, neutrophil; LYMPH, lymphocyte; MONO, monocyte; HGB, hemoglobin; HCT, hematocrit; RBC, red blood cell; PCA, principal component analysis; PLS-DA, partial least squares-discriminant analysis; OPLS-DA, orthogonal partial least squares-discriminant analysis; TNF- $\alpha$ , tumor necrosis factor- $\alpha$ ; IL-2, interleukin-2; IL-1 $\beta$ , interleukin-1 $\beta$ ; IL-18, interleukin-18; IFN- $\gamma$ , interferon- $\gamma$ ; IL-17A, interleukin-17A; IL-10, interleukin-10; Treg, regulatory T; Th17, T helper type 17; Th1, T helper type 1; Th2, T helper type 2; VIP, variable importance in projection; FC, fold change; HMDB, Human Metabolome Database; PG, phosphatidylglycerol; PS, phosphatidylserine; ELISA, enzyme-linked immunosorbent assay.

## Data Sharing Statement

The data used to support the findings of this study are available from the corresponding author upon request.

## Ethical Approval and Informed Consent

All experimental animal protocols were passed by the Institutional Animal Care and Use Committee of Sun Yat-sen University, Guangzhou, China (Ethical Approval No. IACUC 20140515171141).

## Acknowledgments

We gratefully thank Jinqiang Liang (Center of Laboratory Animals, Sun Yat-sen University, Guangzhou, People's Republic of China) for his help and support in animal experiment.

## Funding

This work was supported through the National Science and Technology Major Projects of China (2019ZX09301120).

## Disclosure

Keai Sinn Tan and Wen Tan are employees of Yuanzhi Health Technology Co, Ltd. The authors declare no other potential conflicts of interest for this work.

## References

1. Chang JT. Pathophysiology of inflammatory bowel diseases. *N Engl J Med*. 2020;383:2652–2664. doi:10.1056/NEJMra2002697
2. Auerbach M, Gafter-Gvili A, Macdougall IC. Intravenous iron: a framework for changing the management of iron deficiency. *Lancet Haematol*. 2020;7:e342–e350. doi:10.1016/S2352-3026(19)30264-9
3. Zhao M, Gonczi L, Lakatos PL, Burisch J. The burden of inflammatory bowel disease in Europe in 2020. *J Crohn's & Colitis*. 2021;15:1573–1587.
4. Ahlawat S, Kumar P, Mohan H, Goyal S, Sharma KK. Inflammatory bowel disease: tri-directional relationship between microbiota, immune system and intestinal epithelium. *Crit Rev Microbiol*. 2021;47:254–273. doi:10.1080/1040841X.2021.1876631
5. Aden K, Rehman A, Waschina S, et al. Metabolic functions of gut microbes associate with efficacy of tumor necrosis factor antagonists in patients with inflammatory bowel diseases. *Gastroenterology*. 2019;157:1279–1292. doi:10.1053/j.gastro.2019.07.025
6. Leppkes M, Neurath MF. Cytokines in inflammatory bowel diseases-update 2020. *Pharmacol Res*. 2020;158:104835. doi:10.1016/j.phrs.2020.104835
7. Na YR, Stakenborg M, Seok SH, Matteoli G. Macrophages in intestinal inflammation and resolution: a potential therapeutic target in IBD. *Nat Rev Gastroenterol Hepatol*. 2019;16:531–543. doi:10.1038/s41575-019-0172-4
8. Zhou X, Li W, Wang S, et al. YAP aggravates inflammatory bowel disease by regulating M1/M2 macrophage polarization and gut microbial homeostasis. *Cell Rep*. 2019;27:1176–1189. doi:10.1016/j.celrep.2019.03.028
9. Hall CHT, Lee JS, Murphy EM, et al. Creatine transporter, reduced in colon tissues from patients with inflammatory bowel diseases, regulates energy balance in intestinal epithelial cells, epithelial integrity, and barrier function. *Gastroenterology*. 2020;159:984–998. doi:10.1053/j.gastro.2020.05.033
10. Gui X, Li J, Ueno A, Iacucci M, Qian J, Ghosh S. Histopathologic features of inflammatory bowel disease are associated with different CD4+ T cell subsets in colonic mucosal lamina propria. *J Crohn's & Colitis*. 2018;12:1448–1458.
11. Jang YJ, Kim W-K, Han DH, Lee K, Ko G. Lactobacillus fermentum species ameliorate dextran sulfate sodium-induced colitis by regulating the immune response and altering gut microbiota. *Gut Microbes*. 2019;10:696–711. doi:10.1080/19490976.2019.1589281
12. Friedrich M, Pohin M, Powrie F. Cytokine networks in the pathophysiology of inflammatory bowel disease. *Immunity*. 2019;50:992–1006. doi:10.1016/j.immuni.2019.03.017
13. Nakase H, Uchino M, Shinzaki S, et al. Evidence-based clinical practice guidelines for inflammatory bowel disease 2020. *J Gastroenterol*. 2021;56:489–526. doi:10.1007/s00535-021-01784-1
14. Dart RJ, Ellul P, Scharl M, Lamb CA; Scientific Workshop Steering C. Results of the seventh scientific workshop of ECCO: precision medicine in IBD-challenges and future directions. *J Crohn's & Colitis*. 2021;15:1407–1409.
15. Magro F, Cordeiro G, Dias AM, Estevinho MM. Inflammatory bowel disease-non-biological treatment. *Pharmacol Res*. 2020;160:105075. doi:10.1016/j.phrs.2020.105075
16. Naganuma M, Sugimoto S, Mitsuyama K, et al. Efficacy of indigo naturalis in a multicenter randomized controlled trial of patients with ulcerative colitis. *Gastroenterology*. 2018;154:935–947. doi:10.1053/j.gastro.2017.11.024

17. Jing W, Dong S, Luo X, et al. Berberine improves colitis by triggering AhR activation by microbial tryptophan catabolites. *Pharmacol Res.* 2021;164:105358. doi:10.1016/j.phrs.2020.105358
18. Zhang Y, Yan T, Sun D, et al. Rutaecarpine inhibits KEAP1-NRF2 interaction to activate NRF2 and ameliorate dextran sulfate sodium-induced colitis. *Free Radic Biol Med.* 2020;148:33–41. doi:10.1016/j.freeradbiomed.2019.12.012
19. Fiocchi C, Dragoni G, Iliopoulos D, et al. Results of the seventh scientific workshop of ECCO: precision medicine in IBD—what, why, and how. *J Crohn's Colitis.* 2021;1–65.
20. Gallagher K, Cateson A, Griffin JL, Holmes E, Williams HRT. Metabolomic analysis in inflammatory bowel disease: a systematic review. *J Crohn's Colitis.* 2021;15:813–826. doi:10.1093/ecco-jcc/jjaa227
21. Ding NS, McDonald JAK, Perdones-Montero A, et al. Metabonomics and the gut microbiome associated with primary response to anti-TNF therapy in Crohn's disease. *J Crohn's Colitis.* 2020;14:1090–1102. doi:10.1093/ecco-jcc/jjaa039
22. Tang S-G, Liu X-Y, Ye J-M, et al. Isosteviol ameliorates diabetic cardiomyopathy in rats by inhibiting ERK and NF- $\kappa$ B signaling pathways. *J Endocrinol.* 2018;238:47–60. doi:10.1530/JOE-17-0681
23. Hu H, Sun X, Tian F, Zhang H, Liu Q, Tan W. Neuroprotective effects of isosteviol sodium injection on acute focal cerebral ischemia in rats. *Oxid Med Cell Longev.* 2016;2016:1379162. doi:10.1155/2016/1379162
24. Chen Y, Beng H, Su H, et al. Isosteviol prevents the development of isoprenaline induced myocardial hypertrophy. *Int J Mol Med.* 2019;44:1932–1942. doi:10.3892/ijmm.2019.4342
25. Li T, Wang C, Liu Y, et al. Neutrophil extracellular traps induce intestinal damage and thrombotic tendency in inflammatory bowel disease. *J Crohn's Colitis.* 2020;14:240–253. doi:10.1093/ecco-jcc/jjz132
26. Shen FC, Zhang HJ, Zhao XD, Cao RS, Shi RH. Purine analogues compared with mesalamine or 5-ASA for the prevention of post-operative recurrence in Crohn's disease: a meta-analysis. *Int J Clin Pract.* 2012;66:758–766. doi:10.1111/j.1742-1241.2012.02965.x
27. Assa A, Matar M, Turner D, et al. Proactive monitoring of Adalimumab trough concentration associated with increased clinical remission in children with Crohn's disease compared with reactive monitoring. *Gastroenterology.* 2019;157:985–996. doi:10.1053/j.gastro.2019.06.003
28. Colombel JF, Loftus EV, Tremaine WJ, et al. The safety profile of infliximab in patients with Crohn's disease: the Mayo clinic experience in 500 patients. *Gastroenterology.* 2004;126:19–31. doi:10.1053/j.gastro.2003.10.047
29. Wang S, Tan KS, Beng H, et al. Protective effect of isosteviol sodium against LPS-induced multiple organ injury by regulating of glycerophospholipid metabolism and reducing macrophage-driven inflammation. *Pharmacol Res.* 2021;172:105781. doi:10.1016/j.phrs.2021.105781
30. Zhang H, Lu M, Zhang X, et al. Isosteviol sodium protects against ischemic stroke by modulating microglia/macrophage polarization via disruption of GAS5/miR-146a-5p sponge. *Sci Rep.* 2019;9:12221. doi:10.1038/s41598-019-48759-0
31. Dawson PA, Huxley S, Gardiner B, et al. Reduced mucin sulfonation and impaired intestinal barrier function in the hyposulfataemic NaSI null mouse. *Gut.* 2009;58:910–919. doi:10.1136/gut.2007.147595
32. Wang S, Liu F, Tan KS, et al. Effect of (R)-salbutamol on the switch of phenotype and metabolic pattern in LPS-induced macrophage cells. *J Cell Mol Med.* 2019;24:722–736. doi:10.1111/jcmm.14780
33. Broeckling CD, Prenni JE. Stacked injections of biphasic extractions for improved metabolomic coverage and sample throughput. *Anal Chem.* 2018;90:1147–1153. doi:10.1021/acs.analchem.7b03654
34. Ashrafi F, Kowsari F, Darakhshandeh A, Adibi P. Composite lymphoma in a patient with ulcerative colitis: a case report. *Int J Hematol Oncol Stem Cell Res.* 2014;8:45–48.
35. Chassaing B, Ley RE, Gewirtz AT. Intestinal epithelial cell toll-like receptor 5 regulates the intestinal microbiota to prevent low-grade inflammation and metabolic syndrome in mice. *Gastroenterology.* 2014;147:1363–1377. doi:10.1053/j.gastro.2014.08.033
36. Kobia FM, Preusse K, Dai Q, et al. Notch dimerization and gene dosage are important for normal heart development, intestinal stem cell maintenance, and splenic marginal zone B-cell homeostasis during mite infestation. *PLoS Biol.* 2020;18:e3000850. doi:10.1371/journal.pbio.3000850
37. Zhang A, Sun H, Wang X. Mass spectrometry-driven drug discovery for development of herbal medicine. *Mass Spectrom Rev.* 2018;37:307–320. doi:10.1002/mas.21529
38. Johnson CH, Ivanisevic J, Siuzdak G. Metabolomics: beyond biomarkers and towards mechanisms. *Nat Rev Mol Cell Biol.* 2016;17:451–459. doi:10.1038/nrm.2016.25
39. Brand S. Crohn's disease: Th1, Th17 or both? The change of a paradigm: new immunological and genetic insights implicate Th17 cells in the pathogenesis of Crohn's disease. *Gut.* 2009;58:1152–1167. doi:10.1136/gut.2008.163667
40. Mehandru S, Colombel JF. The intestinal barrier, an arbitrator turned provocateur in IBD. *Nat Rev Gastroenterol Hepatol.* 2021;18:83–84. doi:10.1038/s41575-020-00399-w
41. Tang B, Zhu J, Zhang B, et al. Therapeutic potential of triptolide as an anti-inflammatory agent in dextran sulfate sodium-induced murine experimental colitis. *Front Immunol.* 2020;11:592084. doi:10.3389/fimmu.2020.592084
42. Yang H, Cai R, Kong Z, et al. Teasaponin ameliorates murine colitis by regulating gut microbiota and suppressing the immune system response. *Front Med.* 2020;7:584369. doi:10.3389/fmed.2020.584369
43. Li Y, Pan X, Yin M, Li C, Han L. Preventive effect of lycopene in dDextran sulfate sodium-induced ulcerative colitis mice through the regulation of TLR4/TRIF/NF- $\kappa$ B signaling pathway and tight junctions. *J Agric Food Chem.* 2021;69:13500–13509. doi:10.1021/acs.jafc.1c05128
44. Lee MW, Pourmorady JS, Laine L. Use of fecal occult blood testing as a diagnostic tool for clinical indications: a systematic review and meta-analysis. *Am J Gastroenterol.* 2020;115:662–670. doi:10.14309/ajg.0000000000000495
45. Basseri RJ, Nemeth E, Vassilaki ME, et al. Hepcidin is a key mediator of anemia of inflammation in Crohn's disease. *J Crohn's Colitis.* 2013;7:e286–e291. doi:10.1016/j.crohns.2012.10.013
46. Breugelmanns T, Van Spaendonck H, De Man JG, et al. In-depth study of transmembrane mucins in association with intestinal barrier dysfunction during the course of T cell transfer and DSS-induced colitis. *J Crohn's Colitis.* 2020;14:974–994. doi:10.1093/ecco-jcc/jjaa015
47. Koelink PJ, Bloemendaal FM, Li B, et al. Anti-TNF therapy in IBD exerts its therapeutic effect through macrophage IL-10 signalling. *Gut.* 2020;69:1053–1063. doi:10.1136/gutjnl-2019-318264
48. Joosten LA, Netea MG, Dinarello CA. Interleukin-1 $\beta$  in innate inflammation, autophagy and immunity. *Semin Immunol.* 2013;25:416–424. doi:10.1016/j.smim.2013.10.018
49. Kaplanski G. Interleukin-18: biological properties and role in disease pathogenesis. *Immunol Rev.* 2018;281:138–153. doi:10.1111/imr.12616
50. Mu Q, Chen L, Gao X, et al. The role of iron homeostasis in remodeling immune function and regulating inflammatory disease. *Sci Bull.* 2021;66:1806–1816. doi:10.1016/j.scib.2021.02.010
51. Xu S, He Y, Lin L, Chen P, Chen M, Zhang S. The emerging role of ferroptosis in intestinal disease. *Cell Death Dis.* 2021;12:1–12. doi:10.1038/s41419-020-03229-8
52. Leuti A, Fazio D, Fava M, Piccoli A, Oddi S, Maccarrone M. Bioactive lipids, inflammation and chronic diseases. *Adv Drug Deliv Rev.* 2020;159:133–169. doi:10.1016/j.addr.2020.06.028
53. Collison LW, Murphy EJ, Jolly CA. Glycerol-3-phosphate acyltransferase-1 regulates murine T-lymphocyte proliferation and cytokine production. *Am J Physiol Cell Physiol.* 2008;295:C1543–C1549. doi:10.1152/ajpcell.00371.2007

54. Solverson P, Murali SG, Brinkman AS, et al. Glycomacropptide, a low-phenylalanine protein isolated from cheese whey, supports growth and attenuates metabolic stress in the murine model of phenylketonuria. *Am J Physiol Endocrinol Metab.* 2012;302:E885–E895. doi:10.1152/ajpendo.00647.2011
55. Yu LM, Zhao KJ, Wang SS, Wang X, Lu B. Gas chromatography/mass spectrometry based metabolomic study in a murine model of irritable bowel syndrome. *World J Gastroenterol.* 2018;24:894–904. doi:10.3748/wjg.v24.i8.894
56. Zhou ZY, Zhao WR, Xiao Y, Zhang J, Tang JY, Lee SM. Mechanism study of the protective effects of sodium tanshinone IIA sulfonate against atorvastatin-induced cerebral hemorrhage in zebrafish: transcriptome analysis. *Front Pharmacol.* 2020;11:551745. doi:10.3389/fphar.2020.551745
57. von Martels JZH, Bourgonje AR, Klaassen MAY, et al. Riboflavin supplementation in patients with Crohn's disease [the RISE-UP study]. *J Crohn's Colitis.* 2020;14:595–607. doi:10.1093/ecco-jcc/jjz208
58. Salvador P, Macias-Ceja DC, Gisbert-Ferrandiz L, et al. CD16+ macrophages mediate fibrosis in inflammatory bowel disease. *J Crohn's Colitis.* 2018;12:589–599. doi:10.1093/ecco-jcc/jjx185
59. Yang F, Wang D, Li Y, et al. Th1/Th2 balance and Th17/Treg-mediated immunity in relation to murine resistance to dextran sulfate-induced colitis. *J Immunol Res.* 2017;2017:7047201. doi:10.1155/2017/7047201
60. Pushparaj PN, Li D, Komai-Koma M, et al. Interleukin-33 exacerbates acute colitis via interleukin-4 in mice. *Immunology.* 2013;140:70–77. doi:10.1111/imm.12111
61. Lee S, Park K, Kim J, Min H, Seong RH. Foxp3 expression in induced regulatory T cells is stabilized by C/EBP in inflammatory environments. *EMBO Rep.* 2018;19:e45995. doi:10.15252/embr.201845995
62. Das P, Goswami P, Das TK, et al. Comparative tight junction protein expressions in colonic Crohn's disease, ulcerative colitis, and tuberculosis: a new perspective. *Virchows Arch.* 2012;460:261–270. doi:10.1007/s00428-012-1195-1
63. Rosing N, Salvador E, Guntzel P, et al. Neuroprotective effects of isosteviol sodium in murine brain capillary cerebellar endothelial cells (cerebEND) after Hypoxia. *Front Cell Neurosci.* 2020;14:573950. doi:10.3389/fncel.2020.573950
64. Zhao L, Xiong Q, Sary CM, et al. Bidirectional gut-brain-microbiota axis as a potential link between inflammatory bowel disease and ischemic stroke. *J Neuroinflammation.* 2018;15:1–11. doi:10.1186/s12974-018-1382-3

Journal of Inflammation Research

Dovepress

## Publish your work in this journal

The Journal of Inflammation Research is an international, peer-reviewed open-access journal that welcomes laboratory and clinical findings on the molecular basis, cell biology and pharmacology of inflammation including original research, reviews, symposium reports, hypothesis formation and commentaries on: acute/chronic inflammation; mediators of inflammation; cellular processes; molecular

mechanisms; pharmacology and novel anti-inflammatory drugs; clinical conditions involving inflammation. The manuscript management system is completely online and includes a very quick and fair peer-review system. Visit <http://www.dovepress.com/testimonials.php> to read real quotes from published authors.

Submit your manuscript here: <https://www.dovepress.com/journal-of-inflammation-research-journal>